

COORDINATION CHEMISTRY OF THIOETHER LIGANDS

CENTRE FOR NEWFOUNDLAND STUDIES

**TOTAL OF 10 PAGES ONLY
MAY BE XEROXED**

(Without Author's Permission)

HUIKANG WU, B.Sc.





National Library
of Canada

Bibliothèque nationale
du Canada

Canadian Theses Service

Service des thèses canadiennes

Ottawa, Canada
K1A 0N4

NOTICE

The quality of this microform is heavily dependent upon the quality of the original thesis submitted for microfilming. Every effort has been made to ensure the highest quality of reproduction possible.

If pages are missing, contact the university which granted the degree.

Some pages may have indistinct print especially if the original pages were typed with a poor typewriter ribbon or if the university sent us an inferior photocopy.

Reproduction in full or in part of this microform is governed by the Canadian Copyright Act, R.S.C. 1970, c. C-30, and subsequent amendments.

AVIS

La qualité de cette microforme dépend grandement de la qualité de la thèse soumise au microfilmage. Nous avons tout fait pour assurer une qualité supérieure de reproduction.

S'il manque des pages, veuillez communiquer avec l'université qui a conféré le grade.

La qualité d'impression de certaines pages peut laisser à désirer, surtout si les pages originales ont été dactylographiées à l'aide d'un ruban usé ou si l'université nous a fait parvenir une photocopie de qualité inférieure.

La reproduction, même partielle, de cette microforme est soumise à la Loi canadienne sur le droit d'auteur, SRC 1970, c. C-30, et ses amendements subséquents.

Coordination Chemistry of Thioether Ligands

by

©Huikang Wu, B. Sc.

A thesis submitted to the School of Graduate

Studies in partial fulfillment of the

requirements for the degree of

Master of Science

Department of Chemistry

Memorial University of Newfoundland

St. John's, Newfoundland

CANADA A1B 3X7

1992

ABSTRACT

A series of thiophene-containing thioethers (L1 = 1, 6-bis(2-thienyl)-2,5-dithiahexane; L2 = 1, 9-bis(2-thienyl)-2,5,8-trithianonane; L3 = 1, 9-bis(2-thienyl)-2,8-dithia-5-oxononane; L4 = 1, 7-bis(2-thienyl)-2,6-dithiaheptane) were prepared. Preparation of copper(II), copper(I), molybdenum(0), and tungsten(0) complexes with these ligands and L5 (L5 = 2,5,7,10-tetrathia[12](2,5) thiophenophane) are described. The complexes were studied by nmr, esr, ir, electronic spectroscopy and by magnetic, X-ray structural and electrochemical methods. The structure and properties of the copper complexes were studied in both the solid state and in solution and the structures were correlated with the spectroscopic characteristics. It has been shown that the structures of the copper-thioether complexes change when they dissolve and the extent of the change depends on the solvent and the solution concentrations. Variable temperature nmr studies have been used to examine the stereochemically non-rigid processes of molybdenum and tungsten carbonyl complexes of several of the ligands. At room temperature, all are undergoing rapid inversion of configuration at their metal-bound sulfurs by a solvent-independent process. No evidence of any 1,4-heteroatom fluxional processes was found at room temperature, but at elevated temperatures an unprecedented acyclic 1,4-heteroatom binding site fluxionality in $\text{Mo}(\text{CO})_4 \cdot \text{L2}$ has been observed. The molecular structures of $\text{CuCl}_2 \cdot 2\text{L1}$, $\text{CuCl}_2 \cdot \text{L3}$, $\text{CuBr} \cdot \text{L3}$, and $\text{W}(\text{CO})_4 \cdot \text{L5}$ have been determined by X-ray methods.

ACKNOWLEDGEMENTS

The work described in this thesis was carried out under the supervision of Dr. C.R. Lucas, to whom I am much indebted for advice and encouragement, and for the opportunity of studying under his direction. Assistance by Dr. C.R. Jablonski with nmr spectroscopic measurements, by Dr. J.N. Bridson with the X-ray structural determinations and by Dr. B. Gregory with mass spectroscopy is also gratefully acknowledged. My thanks are also due to Dr. L.K. Thompson and Dr. P.G. Pickup for providing access to conductance and electrochemical equipment. Financial assistance from NSERC (Canada) and from the Department of Chemistry and the school of Graduate Studies of Memorial University of Newfoundland are greatly appreciated.

Sincere gratitude is expressed to my parents in China whom I have missed and who have been constantly in my thoughts. I would also like to thank my wife for her patience and help and for her delicate care of our little son.

Contents

Abstract	ii
Acknowledgement	iii
List of Tables	vii
List of Figures	ix
Abbreviations	xi
1 INTRODUCTION AND SYNTHESIS OF LIGANDS	1
1.1 Introduction	1
1.2 Structure of Copper Thioether Complexes	2
1.3 Electrochemical Properties of Copper Thioether Complexes	5
1.4 ESR of Cu(II)-Thioether Complexes	10
1.5 Dynamic Structure of Thioether Complexes	14
1.5.1 Pyramidal Inversion of Sulphur	14
1.5.2 Fluxionality	18
1.6 Synthesis of Ligands	20
1.6.1 Preparation and Characterization	20

1.6.2	Experimental	22
2	Cu(II)- AND Cu(I)-THIOETHER COMPLEXES	26
2.1	Preparation	26
2.2	Structure and Properties of Cu(II)-Thioether Complexes in the Solid State	29
2.2.1	X-ray Structures	29
2.2.2	Esr of Cu(II)-Thioether Complexes in the Solid State	33
2.2.3	Ir and Magnetic Properties of Cu(II)-Thioether Complexes in the Solid State	35
2.3	Properties of Cu(II)-Thioether Complexes in Solution	37
2.3.1	Electronic Spectroscopy	37
2.3.2	Esr of Cu(II)-Thioether Complexes in Solution	38
2.3.3	Electrochemistry of Cu(II)-Thioether Complexes in Solution	43
2.3.4	Conductance Studies	47
2.4	Conclusions	47
2.5	Cu(I)-Thioether Complexes	49
2.5.1	Preparation	49
2.5.2	X-ray Structure of $(\text{CuBr}\cdot\text{L}_3)_2$	49
2.5.3	Electrochemistry	51
2.6	Experimental	56
3	Molybdenum and Tungsten Carbonyl Thioether Compounds	59
3.1	Preparation	59
3.2	Infrared Spectroscopy	62

3.3	X-ray Structure of $W(CO)_4L_5$	64
3.4	Dynamic Structures of Molybdenum and Tungsten Carbonyl Thioether Compounds	66
3.4.1	Inversion of Coordinated Sulfur	66
3.4.2	Fluxionality	78
3.5	Conclusion	80
3.6	Experimental	80
	Bibliography	81
A	Crystallographic Data	92

List of Tables

1.1	Selected Structure Data for Cu-Thioether Complexes	3
1.2	Reduction Potentials for Copper(II) Complexes with Cyclic and Open-Chain Polythiaethers	6
1.3	Esr Data for Some Cu(II) Complexes	13
1.4	Esr and ENDOR Parameters	13
1.5	Effect of Chelate Ring Size upon Sulfur and Selenium Inversion Energies	17
1.6	Activation Energies for 1,3-Metal Shifts in the Complexes $M(CO)_5L$.	19
1.7	Activation Energies for 1, 2 and 1, 3-Metal Shifts in the Complexes $M(CO)_5L$	20
1.8	Analytical Data for Ligands	24
1.9	Nmr Data and Assignments for Ligands	25
2.1	Physical Properties and Analytical Data for Cu-Thioether Complexes	28
2.2	Selected Bond Lengths(\AA) and Angles(deg) of $CuCl_2 \cdot 2L_1$	30
2.3	Selected Bond Lengths(\AA) and Angles(deg) of $CuCl_2 \cdot L_3$	31
2.4	Esr Data for Cu(II)-Thioether Complexes	33
2.5	Electronic Spectral Data of Cu(II)-Thioether Complexes as Nujol Mulls	36
2.6	Electronic Spectra of Cu(II)-Thioether Complexes in Solution	37

2.7	Cyclic Voltammetry Data of Cu(II)-Thioether Complexes in Dichloromethane	45
2.8	Cyclic Voltammetry Data of Cu(II)-Thioether Complexes in Acetonitrile	45
2.9	Physical Properties and Analytical Data for Cu(I)-Thioether Complexes	51
2.10	Selected Bond Lengths(Å) and Angles(deg) of (CuBr·L3) ₂	52
2.11	Cyclic Voltammetry Data of Cu(I)-Thioether Complexes	54
3.1	Physical Properties and Analytical Data for Molybdenum and Tungsten Thioether Complexes	60
3.2	Nmr Data for Molybdenum and Tungsten Thioether Carbonyl Compounds and Assignments	61
3.3	Infrared Data for Carbonyl Region of Molybdenum and Tungsten Compounds in Dichloromethane	62
3.4	Selected Bond Lengths(Å) and Angles for W(CO) ₄ ·L5	64
A.1	Crystallographic Data for CuCl ₂ ·2L1	93
A.2	Crystallographic Data for CuCl ₂ ·L3	94
A.3	Crystallographic Data for CuBr·L3	95
A.4	Crystallographic Data for W(CO) ₄ ·L5	96

List of Figures

1.1	Square Mechanism for Copper Complexes	9
1.2	Dissociation-Recombination Mechanism for Inversion Process	15
1.3	A Planar Intermediate Mechanism for Inversion Process	16
1.4	Thioether Ligands	21
1.5	Preparation of Thioether Ligands	22
1.6	¹ H Nmr of L3	23
2.1	Preparation of Cu(II)-Thioether Complexes	27
2.2	ORTEP Plot of CuCl ₂ ·2L1	30
2.3	ORTEP Plot of CuCl ₂ ·L3	32
2.4	Esr of Polycrystalline Samples of Cu(II)-Thioether Complexes	34
2.5	Proposed Structure for (CuCl ₂ ·L2) ₂	35
2.6	Esr Spectrum of CuCl ₂ ·L3 in Dichloromethane Glass at 77K	39
2.7	Suggested Structure for CuCl ₂ ·L3 in Dichloromethane	39
2.8	Suggested Structure for (CuCl ₂ ·L2) ₂ in Dichloromethane	40
2.9	Suggested Structure for CuCl ₂ ·2L1 in Dichloromethane	40
2.10	Esr of CuCl ₂ ·2L1 in DMF Glass (diluted) at 77 K	41

2.11 The Proposed Structure for Cu(II)-Thioether Complexes in Dilute DMF Solutions (Species 1)	41
2.12 ESR of $\text{CuCl}_2 \cdot 2\text{L1}$ in DMF Glass (concentrated) at 77 K	42
2.13 CV of $\text{CuCl}_2 \cdot \text{L3}$ in Dichloromethane	44
2.14 CV of $\text{CuCl}_2 \cdot \text{L3}$ in Acetonitrile	46
2.15 Onsager Plot for Cu(II)-Thioether Complexes in Acetonitrile	48
2.16 ORTEP Plot of $(\text{CuBr} \cdot \text{L3})_2$	50
2.17 CV of $\text{CuCl} \cdot \text{L2}$ in Acetonitrile	52
2.18 CV of $\text{CuCl} \cdot \text{L2}$ in Dichloromethane	53
2.19 CV of $\text{CuCl} \cdot \text{L4}$ in Dichloromethane	55
3.1 Infrared Spectra for $\text{Mo}(\text{CO})_4 \cdot \text{L1}$ in Dichloromethane	63
3.2 PLUTO Plot for $\text{W}(\text{CO})_4 \cdot \text{L5}$	65
3.3 Conversion of Configuration of $\text{M}(\text{CO})_4 \cdot \text{L}$	67
3.4 Nmr Spectra for $\text{Mo}(\text{CO})_4 \cdot \text{L1}$ in Dichloromethane at Room Temperature	68
3.5 Numbered structure for $\text{M}(\text{CO})_4 \cdot \text{L1}$	69
3.6 Variable Temperature ^1H nmr for $\text{Mo}(\text{CO})_4 \cdot \text{L1}$ in THF	70
3.7 Variable Temperature ^1H nmr Spectra for $\text{Mo}(\text{CO})_4 \cdot \text{L2}$ in d^8 -THF	73
3.8 Numbered Structure for $\text{Mo}(\text{CO})_4 \cdot \text{L2}$	74
3.9 Numbered Structure for $\text{W}(\text{CO})_4 \cdot \text{L5}$	74
3.10 Variable Temperature ^1H nmr for $\text{W}(\text{CO})_4 \cdot \text{L5}$ in d^8 -THF	76
3.11 Variable Temperature ^1H nmr for $\text{Mo}(\text{CO})_4 \cdot \text{L2}$ in d^8 -Toluene Solution	79

List of Abbreviations

- L1: 1,6-bis(2-thienyl)-2,5-dithiahexane (Fig. 1.4, p21)
L2: 1,9-bis(2-thienyl)-2,5,8-trithianonane (Fig. 1.4, p21)
L3: 1,9-bis(2-thienyl)-5-oxa-2,8-dithianonane (Fig. 1.4, p21)
L4: 1,7-bis(2-thienyl)-2,6-dithiaheptane (Fig. 1.4, p21)
L5: 2,5,8,11-tetrathia[12](2,5) thiophenophane (Fig. 3.9, p74)
[9]aneS3: 1, 4, 7-trithiacyclononane
[12]aneS3: 1, 5, 9-trithiacyclododecane
[12]aneS4: 1, 4, 7, 10-tetrathiacyclododecane
[13]aneS3: 1, 4, 7, 10-tetrathiacyclotridecane
[14]aneS4: 1, 4, 8, 11-tetrathiacyclotetradecane[14]aneS4
[15]aneS4: 1, 4, 8, 12-tetrathiacyclopentadecane[14]aneS4
[16]aneS4: 1, 5, 9, 13-tetrathiacyclohexadecane
[15]aneS5: 1, 4, 7, 10,13-pentathiacyclopentadecane
[18]aneS6: 1, 4, 7, 10, 13, 16-hexathiaclooctadecane
[18]aneS6: 1, 4, 7, 11, 14, 17-hexathiacloecosane
bbte: 1, 2-bis(benzylthio)ethane
en: ethylenediamine
etca: (2-(ethylthio)ethyl)amine
mtmpy: 2-((methylthio)methyl)pyridine
mtpa: (3-(methylthio)propyl)amine
pdto: 1,8-bis(2-pyridyl)-3,6-dithiaoctane
CV: cyclic voltammogram

DMF: dimethylformamide

DTH: 1, 6-bis(methyl)-2,5-dithiahexane

Et₂-2, 3, 2-SNNS: CH₃CH₂SCH₂CH₂NHCH₂CH₂CH₂NHCH₂CH₂SCH₂CH₃

Et₂-2, 3, 2-SSSS: CH₃CH₂SCH₂CH₂SCH₂CH₂CH₂SCH₂CH₂SCH₂CH₃

Haent: 2-aminoethanethiol

Hcys₂: L-cysteine ethyl ester

Hpen: DL-penicillamine

H₂sac₂: N,N'-ethylenebis(thioacetylacetone imine)

Me₂-2, 3, 2-SNNS: CH₃SCH₂CH₂NHCH₂CH₂CH₂NHCH₂CH₂SCH₃

2, 2, 2-NNNN: NH₂CH₂CH₂NHCH₂CH₂NHCH₂CH₂NH₂

2, 2, 2-NSNN: NH₂CH₂CH₂SCH₂CH₂NHCH₂CH₂NH₂

2, 2, 2-NSSN: NH₂CH₂CH₂SCH₂CH₂SCH₂CH₂NH₂

2, 3, 2-NSSN: NH₂CH₂CH₂SCH₂CH₂CH₂SCH₂CH₂NH₂

2, 3, 2-SSSS: HSCH₂CH₂NHCH₂CH₂CH₂NHCH₂CH₂SH

ODACN: 1-oxa-4,7-diazacyclononane

TACN: 1, 4, 7-triazacyclononane

THF: tetrahydrofuran

TMS: tetramethyl silane

Chapter 1

INTRODUCTION AND SYNTHESIS OF LIGANDS

1.1 Introduction

This thesis explores certain aspects of thioether coordination chemistry of molybdenum, tungsten and copper.

Man's knowledge of the coordination chemistry of copper has benefited from extensive studies of copper proteins and their synthetic models. In this thesis, the effect of structure on the properties of copper complexes of sulfur donor ligands in the solid state and in solution are examined with particular emphasis on spectroscopic characteristics and redox properties as revealed by electrochemistry. There is an extensive literature on some of these properties although few comparisons between solid state and solution properties are available.

Molybdenum and tungsten have long been considered as efficient elements to catalyse hydrodesulfurization, the detailed mechanism of which is still, however, unknown. The study of low valent molybdenum and tungsten thioether compounds may help to illustrate the mechanism of hydrodesulfurization. In this thesis, studies

of the structure and properties of molybdenum and tungsten carbonyl thioether complexes and in particular the dynamic structures of these compounds studied by variable temperature nmr methods are reported.

A selective review of the pertinent literature follows.

1.2 Structure of Copper Thioether Complexes

Thioether coordination chemistry has been stimulated in recent years by the desire to develop simple low molecular weight models of the active sites in some enzymes which have been shown to contain metal atoms surrounded by one or more thioether or mercaptide sulfurs. In particular, high resolution x-ray structures of plastocyanin and azurin are available [1, 2] which show the coordination sphere about copper(II) to consist of two aromatic nitrogen atoms, a thioether and a mercaptide sulfur in a distorted tetrahedral array and in the case of azurin, a distant oxygen donor as well.

Development of simple thioether coordination chemistry has benefited greatly from the availability of x-ray crystal structure analysis. In the case of copper complexes where redox is possible it is especially interesting to know the structure of both Cu(II) and Cu(I) complexes which have similar inner coordination spheres. In this section, we will discuss the structural properties of thioether-Cu complexes and whenever possible, we will compare the structures of both Cu(I) and Cu(II) complexes of the same ligand. Some relevant structural parameters of selected examples are listed in Table 1.1

As may be seen from Table 1.1, the structures of Cu(II) thioether complexes are variable. The copper(II) species are, however, frequently found to have structures

Table 1.1: Selected Structure Data for Cu-Thioether Complexes

Compound	Geom.	Cu-S (Å)	Ref.
$[\text{Cu}(\text{[9]aneS3})_2]^{2+}$	O_h	2.419(3), 2.426(3), 2.459(3)	[3]
$[\text{Cu}_2(\text{[9]aneS3})_3]^{2+}$	T_d	2.231(1), 2.302(2), 2.325(2), 2.323(1) 2.244(1), 2.336(1), 2.302(1), 2.329(1)	[4]
$[\text{Cu}(\text{[12]aneS4})(\text{H}_2\text{O})]^{2+}$	C_{4v}	2.34(1), 2.30(1), 2.37(1), 2.32(2)	[5]
$[\text{Cu}(\text{[13]aneS4})(\text{H}_2\text{O})]^{2+}$	C_{4v}	2.334(4), 2.333(4), 2.310(5), 2.330(5)	[5]
$[\text{Cu}(\text{[14]aneS4})]^{2+}$	D_{4h}	2.308(1), 2.297(1)	[5, 6, 7]
$[\text{Cu}(\text{[14]aneS4})]^{+}_n$	T_d	2.260(4), 2.338(4), 2.327(4), 2.342(3)	[6, 8]
$[\text{Cu}(\text{[15]aneS5})]^{2+}$	C_{4v}	2.331(2), 2.315(2), 2.289(2), 2.338(2) 2.398(2)	[9]
$[\text{Cu}(\text{[15]aneS5})]^{+}$	T_d	2.338(5), 2.243(5), 2.317(5)	[9]
$[\text{Cu}(\text{[18]aneS6})]^{2+}$	D_{4h}	2.323(1), 2.402(1), 2.635(1)	[10]
$[\text{Cu}(\text{[18]aneS6})]^{+}$	T_d	2.253(2), 2.358(2), 2.360(2)	[10]

based on some form of distortion from octahedral symmetry as expected on the basis of the Jahn-Teller Theorem. For example, $[\text{Cu}(\text{[9]aneS3})_2]^{2+}$, has a tetragonal elongation to two of its six donor sites while $[\text{Cu}(\text{[15]aneS5})]^{2+}$ is square pyramidal. The complex $[\text{Cu}(\text{[14]aneS4})]^{2+}$ has a planar arrangement for its four donors. On the other hand, the copper(I) complexes have structures that are, in general, tetrahedral or distorted tetrahedral. Much effort has been applied to obtain structures of both Cu(II) and Cu(I) complexes with the same thioether ligand, although for a variety of reasons this is not usually easy. There are, however, now several pairs of examples available, such as for example the case of [14]aneS4. In its Cu(II) complex four sulfurs are in a plane and all are coordinated to one copper [7], but for its Cu(I) complex, the geometry is tetrahedral with three sulfurs coming from one ligand and a fourth sulfur from another ligand to give a polymer [6, 8].

The structures of [15]aneS5 species with both Cu(II) and Cu(I) have also been

determined [9]. For Cu(II), the structure is square pyramidal with five sulfurs of the same ligand all coordinated to one Cu with four shorter basal Cu-S distances and one slightly longer apical Cu-S distance. For Cu(I), the structure is distorted tetrahedral, leaving one sulfur not coordinated. This might be considered to represent the minimum structural change necessary upon reduction from Cu(II) to Cu(I).

In addition to changes in the coordination sphere itself, studies of free and complexed ligands reveal that conformational change in the ligand upon coordination is an important factor for those compounds [11, 12, 13, 14, 15, 16, 17, 18]. In the case of crown ether complexes, there is little conformational change required upon complexation and thermodynamically strong complexes are formed. In the case of thioether analogs, however, the conformations before and after complexation are quite different. Energy to accomplish the conformational change must be found and is usually manifest as a thermodynamic penalty in the stability of the complex. Thus the macrocyclic effect which is dominant in crown ether complexes is of much less significance for many macrocyclic thioether complexes. Oxa- and aza-crowns often choose an endodentate conformation such that their lone pairs all point into the cavity, but the analogous thioether crowns often have exodentate conformations [19], as for example in [12]ancS4, [14]ancS4 and [15]ancS5 in which all sulfur atoms have their lone pairs pointed out of the ring [12]. In [18]ancS6, four sulfur atoms choose exo and two choose an endo orientation. The only ligand for which all sulfur atoms are endo, is [9]ancS3 and it shows a much greater coordination chemistry as a result [20, 21, 22, 23, 24, 25, 26, 27, 28, 29]. The factors which determine whether lone pairs are exo or endo are non-bonded interactions elsewhere in the ligand as explained by Cooper [11]. One of the consequences of the exodentate positioning

of electron pairs is that these ligands often tend to bind to different metals forming binuclear or polynuclear complexes instead of mononuclear ones.

Thioether complexes of copper(I) usually have a Cu(I)-S bond length that is much shorter than the sum of the Pauling covalent radii, (2.39Å). In some cases, it is even comparable to that of Cu(II)-S, (2.34Å). This can be interpreted to mean that π -back donation from Cu(I) to S is important. This bond feature has been found for other transition metal complexes by several workers and its interpretation has been supported by spectroscopic studies [30].

1.3 Electrochemical Properties of Copper Thioether Complexes

Copper proteins play an important role in biological electron transfer reactions. Much work has been done to discover the factors influencing electrochemical properties such as half potentials and self exchange rate constants of copper thioether complexes which are in several respects related to the biological systems [31, 32, 33, 34, 35]. The $E_{1/2}$ values obtained from cyclic voltammetric measurements of these model compounds under slow scan conditions approximate the thermodynamic formal potentials of their redox pairs [36].

It has been shown that Cu-thioether complexes have high positive potentials comparable to those of "blue" copper proteins. Rorabacher et al. [32] have studied the redox chemistry of a series of complexes with both cyclic and open chain thioether ligands and all show high positive potentials among which are some of the highest values reported for the Cu(II)-Cu(I) couple (Table 1.2).

It can be concluded that the high potentials are mainly due to the Cu-S bond.

Table 1.2: Reduction Potentials for Copper(II) Complexes, [CuL]²⁺, with Cyclic and Open-Chain Polythiaethers

L	E _{1/2} (V)	Medium ^a	Rcf.
(9)ancS3 ₂	0.61	a	[10]
[12]ancS3	0.789	b	[32]
[12]ancS4	0.723	b	[32]
	0.64	c	[36]
[13]ancS4	0.674	b	[32]
	0.52	c	[36]
[15]ancS4	0.785	b	[32]
	0.64	c	[36]
[16]ancS4	0.798	b	[32]
	0.69	c	[36]
[15]ancS5	0.855	b	[32]
	0.70	c	[36]
[18]ancS6	0.72	a	[10]
[20]ancS6	0.805	b	[32]
[21]ancS6	0.852	b	[32]
2, 2, 2-NNNN	-0.280	b	[32]
2, 2, 2-NSNN	0.356	b	[32]
2, 2, 2-NSSN	0.361	b	[32]
2, 3, 2-NSSN	0.312	b	[32]
Et ₂ -2, 3, 2-SNNS	0.342	b	[32]
Et ₂ -2, 3, 2-SSSS	0.892	b	[32]
Me ₂ -2, 3, 2-SSSS	0.892	b	[32]
2, 3, 2-SSSS	0.842	b	[32]

^aa: vs SCE, MeNO₂; b: vs NHE, 80% MeOH/20%H₂O; c: vs NHE, H₂O

Presumably the π -acid properties of sulfur stabilize low oxidation states of copper as is observed among other transition metal complexes of thioethers [30]. The general sequence of $E_{1/2}$ values for copper complexes is $\text{CuS}_4 > \text{CuN}_2\text{S}_2 > \text{CuN}_4$ [32, 37, 38, 39] which is consistent with the interpretation of the other data suggesting that thioether sulfur stabilizes the Cu(I) state relative to Cu(II) more efficiently than does aromatic or amine nitrogen [32, 40, 41, 42]. The bond angles of copper complexes may be altered by changing the ligand backbone and this permits fine adjustment of potentials. The $E_{1/2}$ values of a series of S₄ cyclic thioether copper complexes have a range of 674-798 mV in methanol-water solution vs NHE [32]. In general, ligands which sterically or electronically destabilize tetragonal Cu(II) and/or enhance the stabilization of Cu(I) can shift the formal Cu(II)-Cu(I) potential to even more positive values [31, 43].

While stressing the importance of bonding in determining the half wave potentials of Cu-thioether complexes, it should not be overlooked that the structure of Cu thioether complexes also has a large effect on the self-exchange rate constant. In a series of copper thioether complexes studied by Rorabacher et al., the k_{11} values all have an approximate magnitude of $10^2 \text{ M}^{-1} \text{ s}^{-1}$ (range 73-470 $\text{M}^{-1}\text{s}^{-1}$) despite differences in coordination geometry, potentials, and related properties of the Cu(II) and Cu(I) species. The only exception is [15]aneS₅ which has a value of $3 \times 10^4 \text{ M}^{-1} \text{ s}^{-1}$ [9]. Although thorough studies relating these data to solution structures have not been conducted, comparison of [14]aneS₄ and [15]aneS₅ complexes shows the importance of the structure factor in affecting the electron transfer rate. Both Cu(II) complexes appear to adopt relatively strain-free tetragonal geometries in which the copper is coplanar with the four donor atoms in $[\text{Cu}[\text{14]aneS}_4]^{2+}$ [5, 7].

In $[\text{Cu}[15]\text{aneS5}]^{2+}$, however, the Cu is sitting above the plane of the four sulfur atoms with the fifth sulfur occupying the apical position of a square pyramid. In the reduced complexes, the structure of $[\text{Cu}[14]\text{aneS4}]^+$ was found to involve rupture of one of the Cu(II)-S bonds leaving the free sulfur to form a coordinate bond to another Cu(I) atom, thereby generating a 3-1 coordination polymer in the solid state [6, 8]. In solution, kinetic evidence shows that the compound is not a polymer [44] and the Cu(I) atom may be coordinated by three sulfur donor atoms and one solvent molecule. This shows that the coordination donor set may be different in solution from that in the solid and that change of structure is required during the electron transfer reaction. For the [15]aneS5 complexes, the square pyramidal Cu(II) complex is easy to convert to distorted tetrahedral Cu(I) by rupturing one Cu-S bond because the Cu(II) is set above the plane of the four sulfur donors. It is important that although there is bond rupture or formation during the electron transfer reaction, no solvent molecule is needed to coordinate to Cu during the process in order to complete its coordination sphere. Thus this molecule has the fastest electron transfer rate among the series of copper thioether complexes studied by Rorabacher et al. because it needs the minimum configuration change from Cu(II) to Cu(I). This may be related to the high electron transfer rates found in copper enzymes where the copper atom at the active site is in a hydrophobic environment and solvent cage rearrangement is not necessary.

From the above discussion, it seems that the high potentials of Cu-thioether complexes are mainly due to the π -acidity of the sulfur atoms which stabilize the Cu(I) state and hence increase the redox potential. While it is not too difficult to devise complexes having high potentials using thioether ligands, it seems more difficult to

control the structure of the complexes so that they need minimum adjustment while changing from Cu(II) to Cu(I) and vice versa. This may explain why these high potential systems have not found wide use as catalysts.

Since the movement of electrons is much more rapid than the movement of atoms (Franck-Condon Principle), it is presumed that atoms must rearrange to the configuration of the transition state prior to the electron-transfer step [36]. This means that the electron transfer process will be kinetically controlled by the configuration of complexes. The Cu(II) and Cu(I) complexes which have the most closely similar structures will also be closest to the transition state and will be expected to have the fastest electron transfer rates. In the absence of subsequent reactions, these electron transfers will be reversible as expected for good catalyst systems.

These concepts have been explored by Rorabacher [36] who has proposed the square mechanism shown in Fig. 1.1 for Cu-thioether complexes of [14]aneS4. He found that by increasing the scan rate, a second oxidation wave becomes observable at a more positive potential. This means the system is becoming more irreversible because the configuration change of the complexes can not follow the electron transfer speed. The same phenomenon can be seen at low temperature because decreased

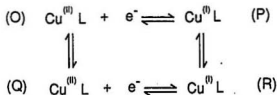


Figure 1.1: Square Mechanism for Copper Complexes

temperature slows the rate of conformation change. In the square mechanism in Fig.1.1, species O and R represent the stable conformers of Cu(II)L and Cu(I)L, respectively, while Q and P are less stable intermediate species. It is presumed that species P represents a Cu(I)L conformer having a coordination geometry more closely approximating the stable conformation of Cu(II)L. Similarly, species Q is presumed to represent a Cu(II)L conformer possessing a coordination geometry more like that of the stable conformation of Cu(I)L. Based on this square scheme, the reduction of Cu(II)L to Cu(I)L may take place by either of two reversible pathways:



The dominant pathway for any Cu(II)L/Cu(I)L system under a specific set of conditions will depend upon the applied potential sweep rate and the relative rate constants for the interconversion of $P \rightleftharpoons R$ and $O \rightleftharpoons Q$. Thus the configuration of complexes is important in controlling the rate of electron transfer and hence the reversibility of the redox system, while control of the thermodynamic parameter, redox potential, is dominated by the donor atom's identity.

From the concepts discussed above, it seems at least theoretically possible to evaluate a homogeneous redox catalyst's kinetic and thermodynamic attributes by studying the electrochemical properties of its solution.

1.4 ESR of Cu(II)-Thioether Complexes

Since it has become widely known that the copper centers in Type I copper proteins have a remarkably small A_{\parallel} value [40, 45, 46, 47], much effort has been made to

correlate the A values with structure and properties of model complexes. From these efforts, considerable experience with the *esr* behaviour of copper complexes has been obtained and certain relationships between g , A and structure have become apparent.

Copper(II) has 9d-electrons, which are always so arranged as to give a total spin $S = 1/2$, no matter what the ligand field is. Thus mono-nuclear Cu(II) complexes present simple systems to be studied by *esr*. From these studies, valuable information about the coordination sphere of a Cu(II) complex can be obtained. The useful parameters are g , A and superhyperfine splitting values. For axial spectra, g is usually split into two components: g_{\perp} and g_{\parallel} . The hyperfine coupling A is also split into two components: A_{\perp} and A_{\parallel} . Usually A_{\perp} is very small so that experimentally it is often not detected or resolved and appears only as a broadening of the g_{\perp} signal. Usually, however, A_{\parallel} is well resolved and can be determined accurately by experiment [48, 49]. For rhombic spectra, one obtains three different g values, g_x , g_y and g_z , although two values, g_x and g_y , may be very close together [48, 49]. The relative values of g_{\parallel} and g_{\perp} are important for determining the shape of the coordination sphere. A bigger g_{\parallel} value indicates square pyramidal or elongated octahedral coordination, whereas bigger g_{\perp} values indicate trigonal bipyramidal or tetragonally compressed octahedral species [48, 49].

For four-coordinated Cu(II) complexes, two extreme structures, square planar and tetrahedral, may be considered. In practice, there are many intermediate structures possible between square planar and tetrahedral and the dihedral angle ω between the two intersecting planes of a tetrahedron is useful in describing the structure. When $\omega = 0^\circ$, the structure is planar and when $\omega = 90^\circ$, it is tetrahedral.

It has been found that in fluid esr spectra, g_0 and A_0 change systematically as a function of ω . As ω increases, both g and $g_{||}$ increase and both A and $A_{||}$ decrease [31, 50]. This has been claimed to be the main factor leading to the small values of $A_{||}$ in blue copper proteins.

For the donor atom N which has a nuclear spin $I = 1$, one can sometimes observe superhyperfine splitting of various features of the esr spectrum. This is helpful for determining whether thioether ligands have dissociated and the complex has been solvated by nitrogen-containing solvents.

The relationship between $A_{||}$ and $g_{||}$ has been known for some time by esr spectroscopists [51]. Plots of $A_{||}$ vs $g_{||}$ for copper complexes with O4, N4, N2S2 or S4 donor sets show clearly the relationship between $A_{||}$ and $g_{||}$ that as $g_{||}$ increases, $A_{||}$ decreases [40, 51].

Another important effect on g values is from the nature of the donor atoms. The following general $g_{||}$ order has been found: O4 > N2O2 > N4 > N2S2 > S4. In other words, sulfur coordinated Cu(II) complexes usually have small g values. For example, $g_{||}$ can change from ca. 2.08 to ca. 2.27 as sulfurs are replaced by oxygens in tetragonal situations [31]. This can be interpreted as evidence of π -acidic properties of thioether sulfur donors. By accepting electron density from the metal ion, thioethers reduce the effective spin-orbit coupling constant and hence the deviation of g from values found with oxygen or nitrogen donor ligands. These effects are illustrated in Table 1.3 for Cu(II) complexes from three different tridentate (N3, N2O and S3) donor sets [52].

Similar results have also been reported for Cu(II)([18]ancS6)(picrate)₂ which has $g_0 = 2.07$ and $A_0 = 0.0064\text{cm}^{-1}$ in nitromethane. In nitromethane-toluene glass it

Table 1.3: ESR Data for Some Cu(II) Complexes

Complex	g_{\parallel}	g_{\perp}	$A_{\parallel} \times 10^4$ (cm^{-1})	$A_{\perp} \times 10^4$ (cm^{-1})	A_{iso} (cm^{-1})	g_{iso}
[Cu(II)(TACN) ₂][Cu(I)(CN) ₃]	2.22	2.05	-177	-22	-75	2.11
[Cu(II)(ODACN) ₂]Br ₂	2.28	2.06	-182	-25		
[Cu(II)(9)ancS3] ₂ (ClO ₄) ₂	2.11	2.02	-153	-20	-62	2.06

Table 1.4: ESR and ENDOR Parameters

Complex	medium	g_{\parallel}	$A_{\parallel} \times 10^4$ (cm^{-1})	$N A \times 10^4$ (cm^{-1})
Cu(pdto)	MeOH	2.177	169	12
Cu(ctea) ₂	H ₂ O/MeOH	2.198	179	10
Cu(mtpa) ₂	H ₂ O/MeOH	2.226	183	10
Cu(pcn) ₂	H ₂ O	2.131	189	9.7
Cu(cyset) ₂	H ₂ O	2.135	189	9.3
Cu(acnt) ₂	H ₂ O	2.129	192	9.0
Cu(mtmpy)	H ₂ O	2.192	159	11
Cu(sacen)	Ni(sacen)	2.108	185	13
Cu(sacen)	Zn(sacen)	2.126	165	12

behaves as an essentially axial complex but with a small rhombic component ($g_x = 2.028$, $g_y = 2.035$, and $g_z = 2.037$, with $A_{\parallel} = 0.0153 \text{ cm}^{-1}$, $A_{\perp} = 0.0019 \text{ cm}^{-1}$). For [Cu[14]ancS4]²⁺, $g_{\parallel} = 2.028$, $g_{\perp} = 2.037$, with $A_{\parallel} = 0.0165 \text{ cm}^{-1}$ and $A_{\perp} = 0.0036 \text{ cm}^{-1}$ [53, 54].

Some other g and A values from the literature are listed in Table 1.4 [55]. The unique bromo- and thioether bridged tetranuclear mixed valence Cu(I)/Cu(II) compound with the N, S-donor ligand 4-((ethylthio)methyl)-5-methyl-imidazole, gives a nearly isotropic signal at $g_{av} = 2.079$. In contrast, and as expected for one unpaired electron residing on the Cu(II) atom, the glass spectrum at 77 K reveals a well-

resolved axial structure ($g_{\parallel} > g_{\perp}$) with the hyperfine parallel components centered at $g = 2.342$ and with $A_{\parallel} = 133$ G [56].

It should be noted that because of the small deviation of g_{\parallel} for Cu(II) thioether complexes from g_e the rules relating g and structure for N and O donor sets must be applied with caution to thioether donor complexes. For example, observation of a g value < 2.03 has been taken previously to indicate compressed tetragonal or trigonal bipyramidal stereochemistry at the Cu(II) ion (i.e. a d_{x^2} ground state) [48], but copper(II)-thioether complexes in general violate this generalization [40]. For example, $[\text{Cu}(\text{18})\text{aneS6}]^{2+}$ has one g value lower than 2.03 but its structure is not compressed tetragonal but rather elongated, as shown by X-ray diffraction [40].

1.5 Dynamic Structure of Thioether Complexes

Abel *et al.* reported the first stereochemically non-rigid sulphur complex in 1966 [57]. It is found that by coordination to transition metals, the pyramidal inversion barrier of sulphur is decreased very much, so that the rate of inversion is within the time scale of nmr. This has resulted in the discovery that pyramidal inversion of coordinated sulfur is widespread and more recently the discovery of binding site fluxionality in sulfur complexes of transition metals. Several reviews are now available [58, 59]. In the following section we will discuss the general features of inversion and fluxional rearrangements in thioether complexes.

1.5.1 Pyramidal Inversion of Sulphur

Pyramidal inversion refers to the spontaneous inversion of configuration of an atom bonded to three substituents in a pyramidal geometry and possessing one lone pair

of electrons. Nitrogen, phosphorus and coordinated thioether sulfur are atoms that exhibit this phenomenon. Inversion was first confirmed for nitrogen atoms [60, 61]. For sulphur, this inversion has a high activation energy barrier and there are only a few reports of pyramidal inversion by organic sulphur compounds [62, 63].

In contrast, the relatively low inversion energy of sulphur when it is coordinated to Pd(II) and Pt(II) was first observed by Abel *et al.*, which triggered many studies on the stereodynamic structure of sulphur atoms.

The big difference in activation energy for sulfur inversion between organic compounds and their metal complexes is due to there being different mechanisms involved [58]. It has been suggested that for inversion to occur in organic compounds, a substituent on sulfur must become detached and subsequently recombined as shown in Fig. 1.2. Examples may be found among the high energy inversions of sulfoxides

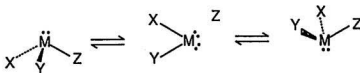


Figure 1.2: Dissociation-Recombination Mechanism for Inversion Process

[62, 63]. For metal complexes of thioethers, due to the strong bond between metal and sulfur, the process in Fig. 1.3 is suggested to involve a planar transition state, which can be stabilized by appreciable (p-d) π back-donation. The ΔG^\ddagger values for inversion of sulfur coordinated to transition metals, as obtained by nmr band fitting programs are in the range of 40 – 70 kJ mol⁻¹ [58, 59]. Platinum and palladium complexes are the most intensively studied but chromium, molybdenum and tungsten complexes have also been examined and the latter tend to show lower activation

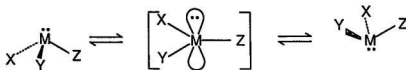


Figure 1.3: A Planar Intermediate Mechanism for Inversion Process

energy barriers to inversion than do the later transition metals.

The nmr method has employed the chiral properties of a sulfur when coordinated to a metal. Thus, the geminal hydrogens on a carbon atom α to the coordinated thioether sulfur are diastereotopic and anisochronous. At low temperature, the nmr of two such hydrogens is an AB quartet which becomes an A_2 singlet as the temperature is raised and inversion at the coordinated sulfur becomes rapid.

Some general conclusions obtained from these nmr studies are:

- Cis complexes of metal dihalides have considerably higher inversion energies than their trans isomers
- The inversion barrier is in the order $\text{Te} > \text{Se} > \text{S}$ and it seems that differences between tellurium and selenium are less than those between selenium and sulfur. For example, the following compounds begin rapid inversion at temperatures as shown [64, 65]:

trans-[PtI ₂ (SEt ₂) ₂]	275 K
trans-[PtI ₂ (SeEt ₂) ₂]	363 K
trans-[PtI ₂ (TeEt ₂) ₂]	378 K

In Table 1.5 are listed some relevant thermodynamic parameters [58, 59].

Table 1.5: Effect of Chelate Ring Size upon Sulfur and Selenium Inversion Energies

Compound	Inversion Energy ΔG^\ddagger (kJ mol ⁻¹)
[PtBrMe ₃ (MeS(CH ₂) ₂ SMe)]	62.8
[PtBrMe ₃ (MeS(CH ₂) ₃ SMe)]	56.6
[PtBrMe ₃ (MeSe(CH ₂) ₂ SMe)]	72.4
[PtBrMe ₃ (MeSe(CH ₂) ₃ SMe)]	64.0
[PtCl ₂ (MeS(CH ₂) ₂ SMe)]	81.4
[PtCl ₂ (MeS(CH ₂) ₃ SMe)]	65.6

- Inversions of sulfur and selenium invariably have lower energies at palladium than at platinum.
- The effect of chelate ring size on both sulfur and selenium inversion has been studied in the series of complexes $\text{trans-[MX}_2\text{(E(CR}_2\text{)}_n\text{)}_2]$ ($M = \text{Pd(II), Pt(II)}$, $X = \text{Cl, Br, I}$; $R = \text{H and/or Me}$; $E = \text{S, Se}$; $n = 2 - 5$) [59].

A steady increase in inversion barrier with decreasing ring size was noted, and the three-membered ring ligand did not undergo inversion before decomposition.

- A trans influence for lowering the inversion energy is obvious. For dialkyl sulfide at platinum(II) it was determined to be $\text{Cl} < \text{Br} < \text{I} < \text{R}_2\text{S} < \text{Ph}$, and it is likely to be essentially inductive in nature.

Finally, it should be noted that because ring conformational change may involve similar energies to those required for inversion, and because such changes may produce the same nmr spectral changes, the simple spin system analysis in early papers on these topics have often confused the two processes. For example, on

studying the temperature dependence of ^1H nmr spectra of metal complexes of 1,2-bis(alkylchalcogeno)ethanes, some authors attributed spectral changes to inversion of configuration at the ligand atoms [66, 67], while others suggested that it arose from conformational changes in the five-membered chelate ring [68]. By the aid of computer synthesised spectra, however, it has been shown that configurational inversion at ligand donor atoms and not conformational reversal of five membered chelate rings is usually responsible for changes of nmr spectra with temperature [69].

1.5.2 Fluxionality

Fluxional movement of ligand atoms on metals is a widespread phenomenon. However, this mainly involves metal-carbon bonds associated particularly with carbonyl and polyenyl ligands. It was not until 1975, that observation of fluxional metal-chalcogen bonds was reported. At that time, Schenk observed a single methyl group signal from $[\text{M}(\text{CO})_5(\overline{\text{SCHMeSCHMeSCHMe}})]$ ($\text{M} = \text{Cr}$ and W) [70] which means that the three sulphurs in the ligand share the metal via 1,3-shifts. Analogous motion was, however, not observed on the unsubstituted ring complexes at the same temperature. The methyl substituent introduces steric factors which favour an axial attachment of $\text{M}(\text{CO})_5$, thereby easing the shift of the $\text{M}(\text{CO})_5$ fragment between adjacent sulfurs. In these complexes of β -2-4-6-trimethyl-1,3,5-trithiane, the metal carbonyl unit is in a fixed axial position so that the axial lone pairs of the uncoordinated sulfur atoms are at a constant distance from it and directed in such a way as to greatly facilitate a 1,3-shift via an easily accessible seven coordinate intermediate. In the unsubstituted trithian complexes, rapid ring reversal and sulfur pyramidal inversion interconverts conformers of similar ground state energy

Table 1.6: Activation Energies for 1,3-Metal Shifts in the Complexes $M(\text{CO})_5\text{-L}$

Compound	ΔG^\ddagger (kJ mole ⁻¹)	Ref.
$[\text{Cr}(\text{CO})_5(\text{SCHMeSCHMeSCHMe})]$	65.80	[76]
$[\text{W}(\text{CO})_5(\text{SCHMeSCHMeSCHMe})]$	68.47	[76]
$[\text{Cr}(\text{CO})_5(\text{SCH}_2\text{SCH}_2\text{SCH}_2)]$	75.80	[77]
$[\text{W}(\text{CO})_5(\text{SCH}_2\text{SCH}_2\text{SCH}_2)]$	78.33	[77]
$[\text{Cr}(\text{CO})_5(\text{SCH}_2\text{SCH}_2\text{SCH}_2\text{SCH}_2)]$	80.62	[59]
$[\text{W}(\text{CO})_5(\text{SCH}_2\text{SCH}_2\text{SCH}_2\text{SCH}_2)]$	83.50	[59]
$[\text{W}(\text{CO})_5(\text{MeSCH}_2\text{SMe})]$	84.3	[78]
$[\text{W}(\text{CO})_5(\text{MeSeCH}_2\text{SeMe})]$	85.8	[78]
$[\text{Cr}(\text{CO})_5(\text{MeSCH}_2\text{SeMe})]^a$	84.5	[78]

^a(Se-Cr bonded)

thus disturbing the ideal relative positioning of the $M(\text{CO})_5$ groups and the sulfur lone pairs. This considerable increase in ligand flexibility reduces the probability of a 1,3-shift occurring [71, 72, 73].

Obviously, steric factors are important in shift processes. Because open chain sulphur ligands will be conformationally more free than cyclic ligands, a higher energy is expected for their fluxional shifts. As ligand ring size increases, flexibility of the ligand increases, the energy of the shift increases and eventually approaches that of open chain ligands. Data for 1,3-shifts on different ligands are listed in Table 1.6.

A change from 1,3-fluxionality to 1,2-fluxionality decreases the distance of metal shift and decreases the energy barrier to the process as can be seen from data in Table 1.7. Logically, one might expect higher energy to be required for a 1,4 shift or alternatively that some assistance such as a pivot point would be necessary. It is therefore not surprising to find that there are in fact only three reports of 1,4 shifts

Table 1.7: Activation Energies for 1, 2 and 1, 3-Metal Shifts in the Complexes $M(CO)_3L$

Compound	ΔG^\ddagger /kJ mole ⁻¹	Ref.
$[Cr(CO)_3(Me_3SiCH_2SSCH_2SiMe_3)]$	70.4	[79]
$[Cr(CO)_3(Me_3SiCH_2SeSeCH_2SiMe_3)]$	75.5	[79]
$[Mo(CO)_3(Me_3SiCH_2SSCH_2SiMe_3)]$	62.6	[79]
$[Mo(CO)_3(Me_3SiCH_2SeSeCH_2SiMe_3)]$	67.1	[79]
$[W(CO)_3(Me_3SiCH_2SSCH_2SiMe_3)]$	74.2	[79]
$[W(CO)_3(Me_3SiCH_2SeSeCH_2SiMe_3)]$	78.4	[79]
$[W(CO)_3(MeSCH_2SMe)]$	84.3	[78]
$[W(CO)_3(MeSeCH_2SeMe)]$	85.8	[78]
$[Cr(CO)_3(MeSCH_2SeMe)]$ (Se-Cr bonded)	84.5	[78]

and all involve cyclic systems [74, 58, 75]. Until this work, there were no reports of 1,4-shifts involving open chain thioether ligands.

1.6 Synthesis of Ligands

1.6.1 Preparation and Characterization

A series of new thiophene-containing thioether ligands (Fig. 1.4) has been prepared by salt elimination reactions of α -chloromethylthiophene with sodium dimercaptans in ethanol as shown in Fig. 1.5. They are all thick liquids at room temperature although L2 can be solidified below 10°C. They all dissolve well in dichloromethane, chloroform, benzene, or diethyl ether, but not in methanol. The ligand L5 (Fig. 3.9) has been reported previously [85].

These ligands were characterized by elemental analyses, mass spectra, ¹H and ¹³C nmr. Low resolution mass spectra have been obtained for all these ligands and while L1 gives a molecular ion peak, L2, L3 and L4 do not. A satisfactory

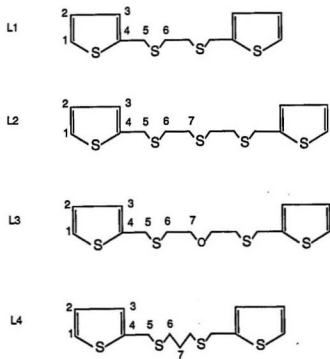


Figure 1.4: Thioether Ligands

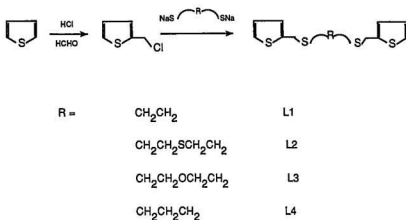


Figure 1.5: Preparation of Thioether Ligands

high resolution mass measurement was obtained for the molecular ion of L1 (The required value is 285.9978 and the found value is 285.9982). Some characterization data are in Tables 1.8 and 1.9 and a representative ^1H nmr spectrum (L3) is shown in Figure 1.6.

1.6.2 Experimental

All commercially available starting materials were obtained from the Aldrich Chemical Co. Inc. and were used without further purification. Preparation of 2-chloromethyl thiophene was carried out according to the reported method [80]. Spectroscopic data were obtained by using the following instruments: Ir, Mattson Polaris FT or Perkin-Elmer Model 283; Nmr, General Electric 300-NB; Mass spectra, V. G. Micromass 7070HS. Analyses were performed by Canadian Microanalytical Service, Ltd. Melt-

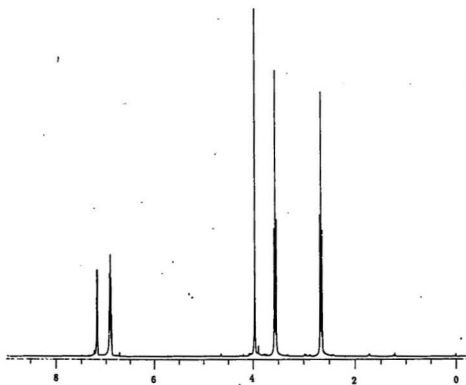


Figure 1.6: ^1H Nmr of L3

Table 1.8: Analytical Data for Ligands

	C(%) (Calc)	H(%) (Calc)	S(%) (Calc)
L2	48.72 (48.55)	5.14 (5.20)	46.24 (46.24)
L3	50.70 (50.91)	5.50 (5.45)	
L4	51.50 (52.00)	5.38 (5.33)	

ing points were determined on a Fisher-John's melting point apparatus and are uncorrected.

General Method for the Preparation of Ligands Sodium (1.15 g, 50.0 mmol) was dissolved in commercial absolute ethanol (150 mL) under a nitrogen atmosphere and the appropriate dimercaptan (25.0 mmol) in ethanol (50 mL) was added dropwise. The resulting mixture was refluxed under nitrogen for about 20 minutes. To the solution, 2-chloromethyl thiophene (6.63 g, 50.0 mmol) in ethanol (50 mL) was added dropwise with stirring. Refluxing was continued for another hour during which time a white precipitate appeared. Water (100 mL) was added. The mixture was extracted with chloroform (3 × 200 mL). The extracts were dried over anhydrous calcium chloride. Volatiles were removed *in vacuo* and the resulting oil was dissolved in a minimum amount of dichloromethane, filtered and methanol added until cloudiness appeared. After cooling to -5°C, formation of a colorless oil occurred and in one case (L2) a white solid formed (m.p.: 10°C). The yields are in the range of 70 - 90 %.

Table 1.9: Nmr Data^a and Assignments for Ligands

Compound	¹ H			¹³ C	Assignment ^c
	δ^b	$^3J_{HH}(Hz)$	$^4J_{HH}(Hz)$	δ^b	
L1	7.14 (m)			124.7	1
	6.85 (m)			125.8,126.3	2,3
				141.3	4
	3.84 (s)			30.7	5
	2.60 (s)			30.2	6
L2	7.21 (m)			124.9	1
	6.91 (m)			125.9,126.5	2,3
				141.4	4
	3.93 (s)			31.2	5
	2.63 (s)			30.4	6
L3	7.18 (dd)	5.1	1.5	124.8	1
	6.90 (m)			126.1,126.5	2,3
				141.8	4
	3.96 (d)		0.5	30.8	5
	3.55 (t)	6.56		70.3	7
	2.65 (t)	6.56		30.7	6
L4	7.13 (q)	4.17	2.15	124.5	1
	6.87 (m)			125.7,126.3	2,3
				141.6	4
	3.84 (s)			30.1	5
	2.51 (t)	7.17		29.9	6
	1.76 (p)	7.17		28.1	7

^ad¹-Chloroform as solvent^bin ppm from TMS; s = singlet, d = doublet, t = triplet, dd = doublet of doublet, p = 5 lines, m = multiplet.^cPosition identification from Fig. 1.4.

Chapter 2

Cu(II)- AND Cu(I)-THIOETHER COMPLEXES

2.1 Preparation

The coordination chemistry of copper has benefited greatly from attempts to model the active sites in "blue" copper proteins. Many model compounds containing Cu-thioether bonds have been prepared in order to compare their properties with those of copper proteins known to contain such bonds [1, S1, S2, S3]. In a similar approach, our thioether ligands were also reacted with copper(II) ion and in most cases, both Cu(II) and Cu(I) complexes were isolated. The structures and properties of the complexes have been studied by infrared spectroscopy, conductivity, electronic spectroscopic and magnetic methods, esr, cyclic voltammetry and X-ray structural methods. Much attention has been paid to changes in structure and to the effects of these changes on the properties of the complexes when in solution. Analytical data and physical properties are given in Table 2.1.

It is worthwhile to discuss these preparations in some detail (Fig. 2.1). When

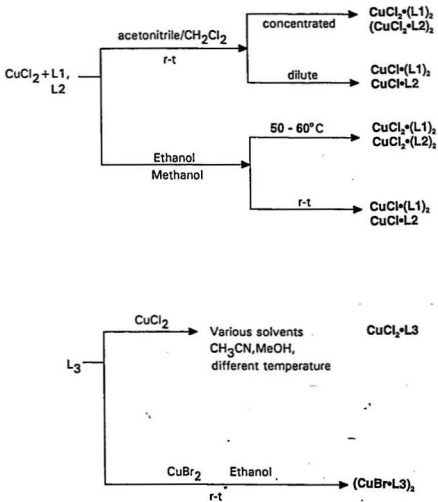


Figure 2.1: Preparation of Cu(II)-Thioether Complexes

Table 2.1: Physical Properties and Analytical Data for Cu-Thioether Complexes

Compound	Color	C(%)(Calc)	H(%)(Calc)	X(%)(calc)	M.P.(°C)	μ_{eff} (B.M.) (25°C)
CuCl ₂ ·(L1) ₂	Brown	40.69 (40.72)	4.10 (3.99)	10.41	91-92	1.87
(CuCl ₂ ·L2) ₂	Brown	34.17 (34.94)	3.62 (3.77)	16.03 (14.75)	112-113	1.88
CuCl ₂ ·L3	Red	36.30 (36.15)	3.91 (3.90)	16.52 (15.26)	115-116	1.48

copper(II) chloride reacts with L1 and L2 (ligands are as defined in chart 1), both Cu(II) and Cu(I) complexes can be isolated depending on the conditions of the reaction. For example, while Cu(II) complexes can be obtained in concentrated acetonitrile/dichloromethane solution at room temperature, dilute solutions give Cu(I) complexes at room temperature. Only Cu(I) complexes can be isolated in ethanol or methanol when L1 and L2 are reacted with copper(II) chloride at room temperature but the Cu(II) complexes can be isolated by carrying out the reaction at high temperature. In ethanol and methanol, with L1 and L2, Cu(II) was reduced, most probably by solvent, to a Cu(I)-thioether complex. Slow evaporation of the acetone solution of the Cu(II) complex of L2 gives twinned crystals. This means that conditions such as solvent and temperature have a great effect on the course of these redox reactions. In contrast to L1 and L2, when L3 is reacted with copper(II) chloride, only Cu(II) complexes can be isolated in solvents such as acetonitrile/dichloromethane, tetrahydrofuran, acetone, methanol or ethanol either at high temperature or room temperature. Allowing these solutions to stand for a long time gives only orange Cu(II) complexes, but not Cu(I) complexes. Even attempted reduction of Cu(II) to

Cu(I) with hypophosphorous acid or reaction of L3 with CuCl, fails to give Cu(I) complexes. As a result, the Cu(I) complex of this ligand can be obtained only from more easily reduced CuBr₂ in ethanol or methanol.

By comparing the preparations of Cu(II) complexes from L1, L2 and L3, it is inferred that the Cu(I) state is stabilized by sulfur donor atoms. On the other hand, the Cu(II) state appears to be stabilized by oxygen atom coordination even if there are some sulfur donors in the complex. It should also be noted that while the Cu(I) state is stabilized by sulfur donor atoms, the Cu(II) complexes are apparently kinetically preferred. Under fast reaction conditions, such as high concentration and high temperature, Cu(II) complexes form, which implies that the redox reaction of these complexes is kinetically determined by a process involving chemical environment change.

The reduction of Cu(II) to Cu(I) is most probably by oxidation of the solvent since the solvent plays a key role in whether Cu(II) or Cu(I) complexes are obtained. The anion apparently also has a significant effect on whether Cu(II) or Cu(I) complexes can be isolated.

2.2 Structure and Properties of Cu(II)-Thioether Complexes in the Solid State

2.2.1 X-ray Structures

CuCl₂·2L1

An ORTEP diagram of CuCl₂·(L1)₂ is given in Fig. 2.2 and Table 2.2 lists selected interatomic distances and bond angles. Crystallographic data is in the Appendix.

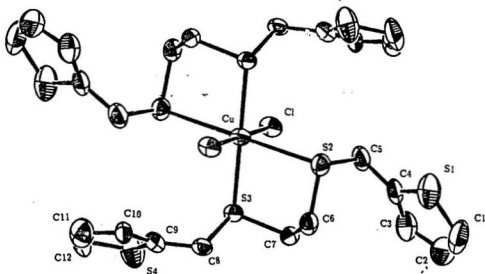


Figure 2.2: ORTEP Plot of $\text{CuCl}_2 \cdot 2\text{L1}$

Table 2.2: Selected Bond Lengths(\AA) and Angles(deg) of $\text{CuCl}_2 \cdot 2\text{L1}$

Bond	Distance	Bonds	Angles(deg)	Bonds	Angles(deg)
Cu-Cl	2.272(1)	S3-Cu-S2	86.10(5)	Cl-Cu-S2	94.43(5)
Cu-S2	2.817(2)	S3-Cu-S2'	93.90(5)	Cl-Cu-S2'	85.57(5)
Cu-S3	2.368(1)	Cl-Cu-S3	85.13(5)	Cl-Cu-S3'	94.87(5)

Table 2.3: Selected Bond Lengths(Å) and Angles(deg) of CuCl₂·L3

Bond	Distance(Å)	Bonds	Angle(deg)	Bonds	Angle(deg)
Cu-Cl1	2.240(4)	Cl1-Cu-Cl2	131.9(2)	Cl1-Cu-O	135.7(3)
Cu-Cl2	2.253(4)	Cl1-Cu-S1	96.08(8)	Cl2-Cu-O	92.4(3)
Cu-O	2.30(1)	Cl2-Cu-S1	92.52(8)	O-Cu-S1	79.44(8)
Cu-S	2.353(2)				

The molecule of CuCl₂·2L1 is centrally symmetric and has a tetragonally elongated pseudo-octahedral coordination sphere with two long trans Cu-S bonds (2.817(2) Å) and two trans Cu-S (2.368(1)Å) as well as two trans Cu-Cl bonds (2.272(1) Å) that are normal in length.

These Cu-S bonds may be compared to those in Cu(CH₃SCH₂CH₂SCH₃)₂(BF₄)₂, (2.317(2) Å) [84], Cu([14]aneS4)(ClO₄)₂, (2.297(1) Å, 2.308(1) Å) [7] or the thiophenophane complexes (CuCl₂·L)₂ (L = C₁₀H₁₄S₄ or C₁₃H₂₀S₅ (2.349(3) – 2.358(3) Å in both) [85] and to the Cu-Cl bonds in the thiophenophane complexes (2.234(3), 2.321(3) and 2.265(4), 2.277(4) Å, respectively). The long trans Cu(II)-S bonds are even longer than the Cu(II)-S distance in Jahn-Teller distorted [Cu([18]aneS6)]²⁺ (2.635(1) Å) [10], but the value 2.817(2) Å is still shorter than 3.20 Å, which is the sum of the van der Waals' radii of copper and sulfur [86].

CuCl₂·L3

The ORTEP drawing of CuCl₂·L3 is shown in Fig. 2.3.

Selected intramolecular distances and angles are listed in Table 2.3. Crystallographic data are in the Appendix. The coordination sphere consists of two chlorines and one oxygen arranged in a triangular plane of symmetry, two sulphurs are in api-

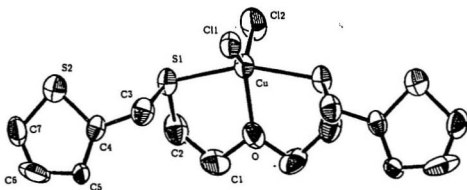


Figure 2.3: ORTEP Plot of $\text{CuCl}_2 \cdot \text{L}_3$

cal positions. The equatorial plane of the distorted trigonal bipyramidal $\text{CuCl}_2 \cdot \text{L}_3$ is a plane of symmetry within which one of the chlorines is displaced $\sim 12^\circ$ from its expected position. The apex-to-apex angle is $\sim 21^\circ$ less than ideal, which may be due to the presence of two five-membered chelate rings that span the apical sites. In support of this, it may be noted that the Cu(II)-S distance is relatively short for apical bonds of this type. In contrast, the Cu-O bond is somewhat longer than expected. For example, the Cu-O bonds are shorter than 2 \AA in all the following complexes: $\text{Cu}(\text{salicylaldehyde})_2$ (form 1), 1.86 \AA and 1.98 \AA , (form2), 1.90 \AA and 1.94 \AA [87, 88], in $\text{Cu}(4\text{-picoline } N\text{-oxide})_2\text{Cl}_2$, $1.949(6) \text{ \AA}$ [89].

Table 2.4: ESR Data for Cu(II)-Thioether Complexes

Compound	medium	g_{\parallel}	g_{\perp}	$A_{\parallel} \times 10^4 (\text{cm}^{-1})$	$A_{\perp} \times 10^4 (\text{cm}^{-1})$
$\text{CuCl}_2 \cdot (\text{L}1)_2$	powder	2.33	2.08	128.7	9.71
	DMF ^a	2.40	2.08		
$\text{CuCl}_2 \cdot \text{L}2$	powder DMF ^a	2.17	2.05	128.3	128.4
		2.39	2.06		
		2.34	2.05		
$\text{CuCl}_2 \cdot \text{L}3$	powder CH_2Cl_2^a	2.04	2.17	142.0	18.0
		2.20	2.04		

^aglass, 77K

2.2.2 ESR of Cu(II)-Thioether Complexes in the Solid State

ESR spectra of polycrystalline samples of $\text{CuCl}_2 \cdot 2\text{L}1$, $(\text{CuCl}_2 \cdot \text{L}2)_2$, and $\text{CuCl}_2 \cdot \text{L}3$ were obtained at 298 and 77K (Fig. 2.4). Values of g_{\parallel} and g_{\perp} are given in Table 2.4. The spectrum of $\text{CuCl}_2 \cdot 2\text{L}1$ is that of a simple axial species ($g_{\parallel} > g_{\perp}$) with no resolved metal hyperfine coupling. It suggests that $d_{x^2-y^2}$ is the ground state of Cu(II) [48, 49] and this is consistent with the structure found in the X-ray study.

The esr of $(\text{CuCl}_2 \cdot \text{L}2)_2$ is similar to that of $\text{CuCl}_2 \cdot 2\text{L}1$ with $g_{\parallel} = 2.174$ and $g_{\perp} = 2.075$. This suggests that in the solid state $(\text{CuCl}_2 \cdot \text{L}2)_2$ has a tetragonally elongated or square pyramidal structure. It is of note that this spectrum is similar to those of dinuclear CuCl_2 complexes of thiophenophanes described previously by Lucas [85] in which chloride behaves as a bridge between two copper centres. Unfortunately, we cannot study the structure of this complex by x-ray methods due to the formation of twinned crystals that are unsuitable for such a study. The structure of this complex, however, can be deduced from spectroscopic data and will be presented in the next Section.

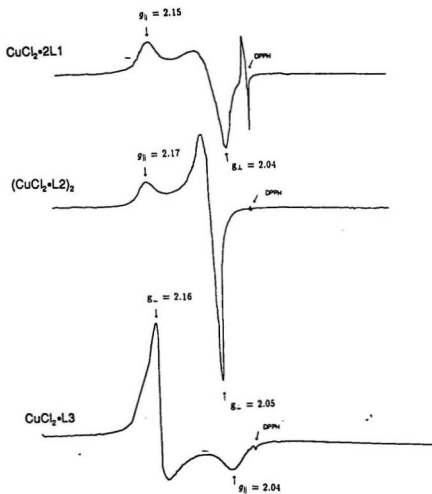


Figure 2.4: ESR of Polycrystalline Samples of Cu(II)-Thioether Complexes

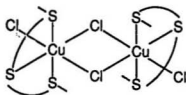


Figure 2.5: Proposed Structure for $(\text{CuCl}_2 \cdot \text{L}_2)_2$

In contrast to $\text{CuCl}_2 \cdot 2\text{L}_1$, and $(\text{CuCl}_2 \cdot \text{L}_2)_2$, $\text{CuCl}_2 \cdot \text{L}_3$ shows a reverse axial spectrum ($g_{\perp} > g_{\parallel}$), suggesting a $d_{x^2-y^2}$ ground state. This coincides with the trigonal bipyramidal structure revealed by X-ray crystallography.

The g values of $\text{CuCl}_2 \cdot \text{L}_3$ ($g_{\perp} = 2.17$, $g_{\parallel} = 2.04$) do not deviate very much from the value of g_e , as is usual for the Cu(II) -thioether complexes [51, 53].

2.2.3 Ir and Magnetic Properties of Cu(II) -Thioether Complexes in the Solid State

Far infrared spectra are sometimes helpful to detect terminal or bridging Cu-Cl bonds. Dinuclear compounds similar to those in this study that have been described previously show strong infrared absorptions at 300 and 250 cm^{-1} , belonging to terminal Cu-Cl and bridging Cu-Cl-Cu vibrations [85, 90]. Although the same bands are found in spectra of $(\text{CuCl}_2 \cdot \text{L}_2)_2$, the 250 cm^{-1} band is either absent or very weak in spectra of $\text{CuCl}_2 \cdot 2\text{L}_1$ and $\text{CuCl}_2 \cdot \text{L}_3$ which leads one to believe that the L_2 complex is a dimer with Cu-Cl-Cu bridges whereas the other complexes are monomers. On the basis of esr and ir evidence, the structure of $(\text{CuCl}_2 \cdot \text{L}_2)_2$ which is proposed is that of a dimer with two chlorine bridges as shown in Fig. 2.5.

Table 2.5: Electronic Spectral Data of Cu(II)-Thioether Complexes as Nujol Mulls

Compound	λ in nm (assignment)		
CuCl ₂ ·2L1	325 LMCT(Cl)	440 LMCT(S)	590 (d→d)
(CuCl ₂ ·L2) ₂	300 LMCT(Cl)	435 LMCT(S)	600 (d→d)
CuCl ₂ ·L3	320 LMCT(Cl)	425 LMCT(S)	790 (d→d)

It is proposed that the two coordination spheres, each of which is five-coordinate, are linked apex-to-base and apex-to-base as shown. In this way, the magnetically active $d_{x^2-y^2}$ orbitals should have minimal interaction with each other and as has been shown previously [85], this should lead to a magnetic moment that is not reduced by antiferromagnetic coupling. The experimental values for μ_{eff} for these compounds are in Table 2.1 and that for (CuCl₂·L2)₂ is consistent with the proposed structure.

Electronic Spectroscopy

The electronic spectra (Table 2.5) of the complexes in the solid state are very similar in the charge transfer region but their ligand field spectra show some differences. The d-d bands of CuCl₂·2L1 and (CuCl₂·L2)₂ are at ca. 600 nm with a long tail to ca. 850 nm, which is consistent with a square pyramidal or distorted octahedral configuration [91]. The d-d band envelope in CuCl₂·L3 is red shifted ~200 nm, however, compared to the other two species which is probably due to the change to trigonal bipyramidal geometry. In other respects the three chromophores behave similarly. Apparently, the weakly bound O-donor in CuCl₂·L3, the weakly bound apical S-donors in CuCl₂·2L1 and the presumably weakly bound axial S-donor in

Table 2.6: Electronic Spectra of Cu(II)-Thioether Complexes in Solution

Compound	λ in nm (ϵ^a)		Assignment
	Dichloromethane	Acetonitrile	
CuCl ₂ ·2L1	330(900)	310(2000)	Cl→Cu
	440(360)	440(600)	S→Cu
	740(70)	730(80)	d→d
	950(sh ^b)		
(CuCl ₂ ·L2) ₂	325(1040)	300(2000)	Cl→Cu
	435(360)	420(700)	S→Cu
	755(85)	725(70)	d→d
	950(sh)		d→d
CuCl ₂ ·L3	330(sh)	300(1500)	Cl→Cu
	435(500)	430(500)	S→Cu
	720(75)	725(65)	d→d
	925(sh)		

^ain cm⁻¹.mol⁻¹.dm³.

^bsh = shoulder

(CuCl₂·L2)₂ have little effect on the spectra. The "effective" chromophore in all three compounds is therefore CuCl₂S₂.

2.3 Properties of Cu(II)-Thioether Complexes in Solution

The spectroscopic characteristics of these complexes were studied in solution and the results suggest that the structures of these complexes change when they pass into solution and that the extent of change depends *inter alia* on the solvent.

2.3.1 Electronic Spectroscopy

Electronic spectroscopic data for the Cu(II)-thioether complexes in dichloromethane

and acetonitrile are collected in Table 2.6. The compounds appear to have a similar "effective" chromophore in solution. For $\text{CuCl}_2\cdot\text{L}3$, the d-d bands are now more like those in $\text{CuCl}_2\cdot 2\text{L}1$, and $(\text{CuCl}_2\cdot\text{L}2)_2$ than was the case in the solid state, suggesting loss of its trigonal bipyramidal structure upon dissolving. This probably results from attack of solvents in the trigonal plane. On changing solvents to acetonitrile, further changes in the d-d bands occur, the most obvious being that the shoulder at ca. 950 nm becomes undetectable. This suggests that there is a structure change, the nature of which is revealed by cyclic voltammetry and conductance studies that will be discussed shortly.

2.3.2 ESR of Cu(II)-Thioether Complexes in Solution

The esr spectrum of $\text{CuCl}_2\cdot\text{L}3$ in dichloromethane glass at 77K is shown in Fig. 2.6. It is an axial spectrum with $g_{\parallel} = 2.22$ and $g_{\perp} = 2.04$ [48, 49]. The hyperfine structure of both parallel and perpendicular regions is well resolved with $A_{\parallel} = 142 \times 10^{-4}$, and $A_{\perp} = 8 \times 10^{-4} \text{ cm}^{-1}$. The structure of $\text{CuCl}_2\cdot\text{L}3$ in dichloromethane is obviously different from that in the solid state. The axial spectrum suggests either an elongated tetragonally distorted octahedral or square pyramidal structure in dichloromethane which is consistent with the conclusions from electronic spectroscopy. It is proposed on the basis of these observations that the structure of $\text{CuCl}_2\cdot\text{L}3$ in dichloromethane is that of a pseudo-octahedral solvate as shown in Fig. 2.7.

Because of their similar electronic and esr spectra, the coordination environments of these Cu(II)-thioether complexes in solution are likely to be similar. For $(\text{CuCl}_2\cdot\text{L}2)_2$, the dimer is probably cleaved into a solvated monomer as shown in Fig. 2.8 while for $\text{CuCl}_2\cdot 2\text{L}1$ cleavage of at least one of the long Cu-S bonds to give



Figure 2.6: Esr Spectrum of $\text{CuCl}_2 \cdot \text{L}_3$ in Dichloromethane Glass at 77K

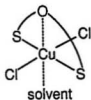


Figure 2.7: Suggested Structure for $\text{CuCl}_2 \cdot \text{L}_3$ in Dichloromethane

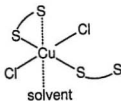


Figure 2.8: Suggested Structure for $(\text{CuCl}_2 \cdot \text{L}_2)_2$ in Dichloromethane

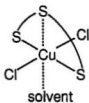


Figure 2.9: Suggested Structure for $\text{CuCl}_2 \cdot 2\text{L}_1$ in Dichloromethane

the species shown in Fig. 2.9 seems probable. As noted for their electronic spectra, change of solvents also affects their esr spectra. In DMF, two species are detectable for all three complexes in dilute solution. A representative spectrum is in Fig. 2.10. Species 1 is detected in solutions of CuCl_2 containing any bidentate thioether ligand and the superhyperfine structure on g_{\perp} suggests interaction with two N atoms ($I = 1$) in the equatorial plane. The structure proposed for Species 1 is shown in Fig. 2.11. Species 2 has the same characteristics as those of anhydrous cupric chloride dissolved in DMF. Under these conditions, cupric chloride is known to dissociate one Cl^- and to exist as a solvate [92]. This means that in a strong donor solvent

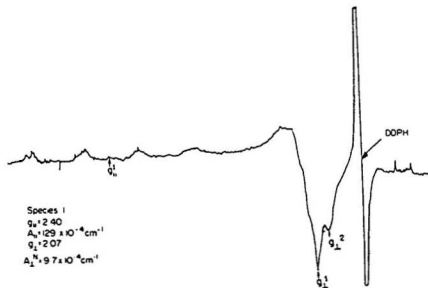


Figure 2.10: ESR of $\text{CuCl}_2 \cdot 2\text{L1}$ in DMF Glass (diluted) at 77 K

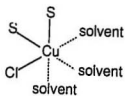


Figure 2.11: The Proposed Structure for Cu(II) -Thioether Complexes in Dilute DMF Solutions (Species 1)

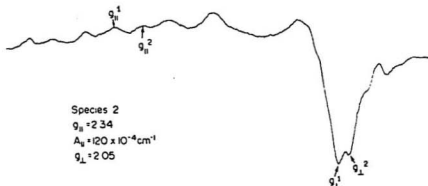


Figure 2.12: ESR of $\text{CuCl}_2 \cdot 2\text{L1}$ in DMF Glass (concentrated) at 77 K

such as DMF, the sulphur donors of these complexes can be replaced by DMF and there is an equilibrium:

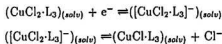


The relative amounts of Species 1 and Species 2 change when the esr is run at different solution concentrations (Figs. 2.10 and 2.12) which is consistent with the presence of an equilibrium such as that shown in the equation above.

2.3.3 Electrochemistry of Cu(II)-Thioether Complexes in Solution

In the preceding section, evidence was presented which suggests that these Cu(II)-thioether complexes change their structure upon dissolving in various solvents. In solvents of poor donor ability such as dichloromethane, it seems that there is only a small geometry change or a dissociation of weakly bonded donors. When solvents of stronger donor ability are used, in addition to dissociation of weakly bonded donors, it is also possible to dissociate more firmly bound ligands such as chlorine. To confirm these tentative conclusions, the complexes were studied by cyclic voltammetry in dichloromethane and acetonitrile.

In dichloromethane, the cyclic voltammograms are characteristic of EC processes. A representative voltammogram for $\text{CuCl}_2 \cdot \text{L}_3$ is shown in Fig. 2.13. Data for all three complexes are in Table 2.7. Processes consistent with the cyclic voltammograms and with the uv and esr data (discussed earlier) are:



Thus the electrochemical reduction proceeds by an initial electron transfer followed by a chloride dissociation. In the initial cathodic sweep of potential, electron transfer occurs. At slow scan rates, for the reverse sweep of potential, the species originally produced in the reduction wave is not available in stoichiometric amounts since some of it has suffered loss of Cl^- . Accordingly, the anodic wave is much reduced. As the scan rate is increased, the anodic wave grows as shown by the change of i_{pa}/i_{pc} . This is due to the fact that at higher scan rates the return sweep occurs

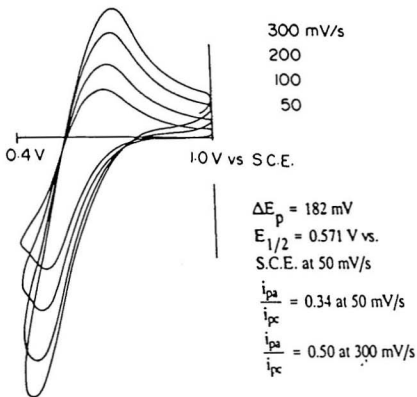


Figure 2.13: CV of $\text{CuCl}_2\text{-L3}$ in Dichloromethane

Table 2.7: Cyclic Voltammetry Data^a of Cu(II)-Thioether Complexes in Dichloromethane

Compound	E _{pc} (mV)	E _{pa} (mV)	ΔE(mV)	E _{1/2} (V)
CuCl ₂ ·2L1	515	672	157	0.594
(CuCl ₂ ·L2) ₂	475	736	261	0.606
CuCl ₂ ·L3	480	662	182	0.571

^aScan rate: 50 mV/s; Electrode: Glassy Carbon—Pt(wire)—SCE; Supporting electrolyte: Et₄NClO₄

Table 2.8: Cyclic Voltammetry Data^a of Cu(II)-Thioether Complexes in Acetonitrile

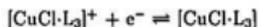
Compound	E _{pc} (mV)	E _{pa} (mV)	ΔE(mV)	E _{1/2} (V)	i _{pa} /i _{pc}
CuCl ₂ ·2L1	460	550	95	0.50	0.97
(CuCl ₂ ·L2) ₂	465	555	90	0.51	1.0
CuCl ₂ ·L3	445	570	125	0.51	1.0

^aScan rate: 50 mV/s; Electrode: Pt(wire)—Pt(wire)—SCE; Supporting electrolyte: Et₄NClO₄

before chloride dissociation is complete.

Changing solvent from dichloromethane to acetonitrile causes a remarkable effect on the cyclic voltammograms of these compounds which in acetonitrile are all similar and characteristic of quasi-reversible processes. A representative example is in Fig. 2.14, while data for all the compounds is in Table 2.8.

A process consistent with the cyclic voltammograms and with the spectroscopic data described earlier is:



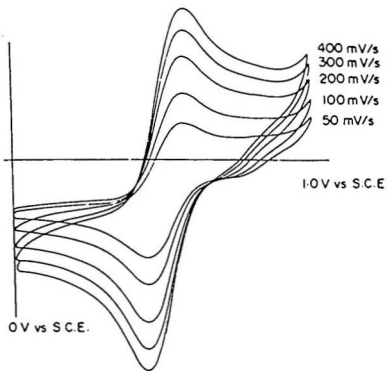


Figure 2.14: CV of $\text{CuCl}_2 \cdot \text{L}_3$ in Acetonitrile

Because of the stronger donor ability of acetonitrile compared to dichloromethane, as shown earlier one of the chlorides on copper is displaced by acetonitrile to give a cationic species which is then reduced in a reversible or quasi-reversible process.

Thus, the complexes exhibit different electrochemical properties in different solvents which indicates different structures exist in the various solvents. In dichloromethane, the structure is similar to that in the solid except for solvation of open coordination sites or cleavage of weak bridge bonds or those to distant ligands, while in acetonitrile, one chloride dissociates.

2.3.4 Conductance Studies

As final confirmation of the conclusions reached on the basis of spectroscopic and electrochemical results, a conductance study in acetonitrile was undertaken. The results are displayed as an Onsager Plot [93] in Fig. 2.15 which reveals the electrolyte type. The slopes of the plots for $(\text{CuCl}_2 \cdot \text{L}_2)_2$ and $\text{CuCl}_2 \cdot \text{L}_3$ clearly indicate these compounds are 1:1 electrolytes in acetonitrile which confirms conclusions reached in earlier sections of this thesis.

The conductance data for $\text{CuCl}_2 \cdot 2\text{L}_1$ are more difficult to interpret than the data for the other two complexes and the Onsager Plot for that compound does not give a straight line but rather a curve between the slopes of 1:1 and 1:2 electrolytes. This could be interpreted to mean that dissociation of a second chloride from copper is also possible for this complex.

2.4 Conclusions

- CuCl_2 and its complexes with O- and S-donors undergo significant structural

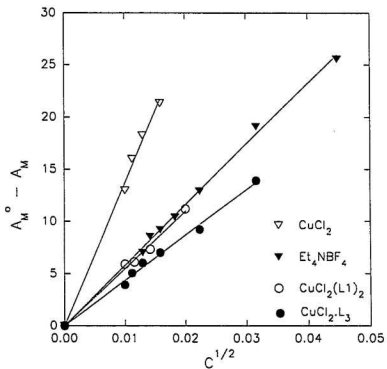


Figure 2.15: Onsager Plot for Cu(II)-Thioether Complexes in Acetonitrile

changes upon being dissolved in various solvents. The nature and extent of these changes depend upon both the characteristics of the solvent and upon the concentration of the solution. In poorly coordinating solvents, ligand donor atoms may be displaced if they are weakly bonded but otherwise they are not displaced. Dimers may be cleaved to monomers and five coordinate species may become six coordinate solvates.

- In more nucleophilic solvents, dissociation of a Cu-Cl bond may occur as may reversible dissociation of Cu-S and Cu-O bonds leading ultimately to $[\text{CuCl}\cdot(\text{solvent})_n]^+$ in dilute solutions.

2.5 Cu(I)-Thioether Complexes

2.5.1 Preparation

As discussed in Section 2.1, all the Cu(I) complexes can also be prepared from Cu(II) salts. Slow evaporation of solutions of copper(II) salts containing appropriate related ligands gives white crystals of copper(I) complexes. Some properties and analytical results are listed in Table 2.9.

2.5.2 X-ray Structure of $(\text{CuBr}\cdot\text{L3})_2$

The molecular structure of $(\text{CuBr}\cdot\text{L3})_2$ has been determined by X-ray crystallography. An ORTEP drawing of the molecule and selected bond lengths and angles are given in Fig. 2.16 and Table 2.10. Crystallographic data are in the Appendix. The Cu-Br bond lengths are 2.533(2) and 2.475(2) Å, which are a little longer than those in $[\text{CuBr}(\text{benzo-}[9]\text{janeS3})]$ (2.322(5), 2.332(5), 2.323(4) Å) [94]. The Cu-S bond lengths in this complex (2.288(3), 2.335(3) Å) are even shorter than that in

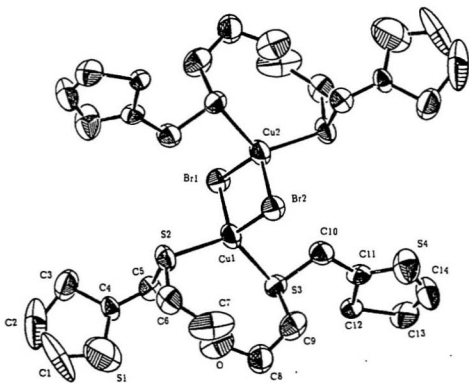


Figure 2.16: ORTEP Plot of $(\text{CuBr-L3})_2$

Table 2.9: Physical Properties and Analytical Data for Cu(I)-Thioether Complexes

	Color	C(% (Calc)	H(% (Calc)	S(% (Calc)	X(% (Calc)	M.P.(°C)
CuCl·(L1) ₂	white	40.44 (42.88)	3.93 (4.26)		5.97 (5.28)	87-90
CuCl·L2	white	37.49 (37.72)	4.05 (4.07)		8.10 (7.96)	132-133
CuSCN·L2		38.29 (38.49)	3.81 (3.88)	40.72 (41.05)		
CuBr·L3·CH ₃ COCH ₃	white	38.32 (38.37)	4.06 (4.55)		15.34 (15.03)	98-100
CuCl·L4	white	38.22 (39.09)	3.90 (4.01)			

the copper(II) complex of L3, CuCl₂·L3 (2.353(2) Å). This is consistent with the expected Cu(I) back donation of electron density to sulphur which strengthens the Cu-S bond and stabilizes the Cu(I) state. The affinity of Cu(I) for sulfur is shown by the fact that the oxygen donor atom which is in the center of the ligand's thioether chain, does not coordinate to copper. Instead of forming a five membered chelate ring, an eight membered ring in which the Cu(I) is coordinated only by thioether sulfur atoms forms.

2.5.3 Electrochemistry

Cyclic voltammetric data are in Table 2.11 and show a strong dependence on solvent. In acetonitrile, the cyclic voltammograms of copper(I) and copper(II) complexes of the same ligand are very similar (See Tables 2.8 and 2.11). A representative voltammogram for CuCl·L2 is shown in Fig. 2.17. This suggests that the species formed by electrochemical reduction of copper(II) and by synthesis from copper(I)

Table 2.10: Selected Bond Lengths(\AA) and Angles(deg) of $(\text{CuBr-L3})_2$

Distances (\AA)			
Cu(1)-Br(1)	2.533(2)	Br(2)-Cu(1)	2.475(2)
Cu(1)-Cu(2)	2.714(3)	Cu(1)-S(3)	2.335(3)
Cu(1)-S(2)	2.288(3)		
Angles (deg)			
Cu(1)-Br(1)-Cu(2)	65.62(6)	Br(1)-Cu(1)-Br(2)	114.38(6)
Br(1)-Cu(1)-Cu(2)	56.17(6)	Br(1)-Cu(1)-S(3)	99.32(9)
Br(1)-Cu(1)-S(2)	103.9(1)	Br(2)-Cu(1)-Cu(2)	58.21(6)
Br(1)-Cu(1)-S(3)	105.85(9)	Br(1)-Cu(1)-S(2)	114.6(1)
Cu(1)-Cu(2)-S(3)	113.6(1)	Cu(1)-Cu(2)-S(2)	127.1(1)

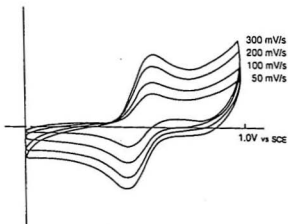


Figure 2.17: CV of CuCl-L2 in Acetonitrile

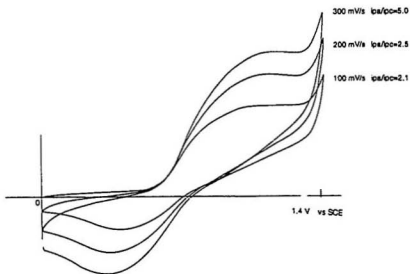


Figure 2.18: CV of $\text{CuCl}\cdot\text{L}_2$ in Dichloromethane

are similar and supports conclusions in Section 2.3.3 concerning solution structures of the copper complexes. In dichloromethane, the cyclic voltammograms of the copper(I) complexes are quite different from those of the copper(II) complexes in the same solvent and both are different from those in acetonitrile (See Tables 2.7 and 2.11). A representative voltammogram for $\text{CuCl}\cdot\text{L}_4$ is shown in Fig. 2.18.

In dichloromethane, the $E_{1/2}$ values obtained from the Cu(I) complexes are significantly higher than those obtained from the analogous Cu(II) complexes, in one case by as much as $\sim 0.15\text{V}$. The ratios of i_{pa}/i_{pc} obtained from the copper(II) complexes in dichloromethane are much smaller than one, while i_{pa}/i_{pc} obtained from

Table 2.11: Cyclic Voltammetry Data^a of Cu(I)-Thioether Complexes

Compound	Solvent ^b	E _{pc} (mV)	E _{pa} (mV)	Δ E (mV)	E _{1/2} (V)	i _{pa}	i _{pc}	i _{pa} /i _{pc}
CuCl·L1	a	470	590	106	0.53	1.15	115	1.0
CuCl·L1	b	560	740	180	0.65			
CuCl·L2	a	485	575	90	0.53	0.70	0.80	0.88
CuCl·L2	b	501	1018	500	0.760			
CuSCN·L2	a	562	618	56	0.59			
CuSCN·L2	b	775	941	166	0.86			
CuBr·L3	a	548	597	51	0.573			
CuBr·L3	b	835	938	103	0.88			
CuCl·L4	a	495	575	80	0.53	0.75	0.75	1.0
CuCl·L4	b	805	925	120	0.865			

^aScan rate: 50 mV/s; Electrode: Pt(wire)—Pt(wire)—SCE; Supporting electrolyte: Et₄NClO₄.

^ba: Acetonitrile; b: Dichloromethane

analogous copper(I) complexes in dichloromethane are much bigger than one. This suggests that the species first formed by electrochemical reduction of copper(II) and the species formed by synthesis from copper(I) are different, and furthermore that the species first formed by electrochemical oxidation of copper(I) and the species formed by synthesis from copper(II) are different. This suggests the EC mechanism as shown below:



Comparing CuCl·L2 with Cu(SCN)·L2, the E_{1/2} is higher for Cu(SCN)·L2 than that for CuCl·L2. This anion effect can be understood in terms of the fact that the SCN⁻ ion is a soft base and Cl⁻ ion is a hard base. Changing from a hard base to a softer one will stabilize the Cu(I) state and thus enhance the Cu(II)/Cu(I) potential.

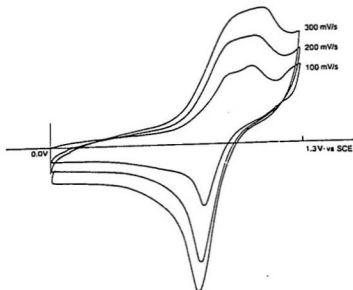


Figure 2.19: CV of CuCl·L4 in Dichloromethane

The anion effect is also observed during preparation of complexes of L3. As pointed out previously, we cannot obtain the Cu(I) complex of L3 from CuCl₂. When CuBr₂ is used, however, the Cu(I) complex is easily obtained.

In dichloromethane, upon decreasing the sweep rate, a second oxidation peak appeared in cyclic voltammograms of CuCl·L1 and CuCl·L4 (Fig. 2.19). This may reflect the existence of an unstable intermediate formed during the electrochemical reaction. This is similar to the explanation by Rorabacher et al. [36] who proposed the "square mechanism" (Fig. 1.1) to account for their observation of two reduction waves. The relative intensities of these two oxidation peaks do not change very much as the sweep rate changes. This may mean that the more stable conformer and

the less stable conformer have reached equilibrium under these conditions. When they are in equilibrium, and electron transfer is rapid for both, two peaks, one corresponding to each conformer, may be seen. This implies that the equilibrium between the two conformers is easily reached, and they therefore need minimum adjustment to interconvert.

2.6 Experimental

All commercially available starting materials were obtained from the Aldrich Chemical Co. Inc. or from Morton Thiokol Alfa Products Inc. and were used without further purification. Electronic spectra were obtained by using a Cary 17 uv/vis spectrophotometer. Magnetic data were obtained at room temperature by the Faraday method using $\text{Hg}[\text{Co}(\text{NCS})_4]$ as calibrant. The susceptibility data were corrected for diamagnetism using Pascal's constants. ESR spectra were recorded at room temperature and 77K on a Bruker ESP-300 X-Band spectrometer at ~ 9.5 GHz. Cyclic voltammograms were recorded on a BAS CV27 Voltammograph and a Houston 2000-Omnigraph X-Y recorder using a glassy carbon working electrode, a platinum counter electrode and an aqueous saturated calomel reference electrode. Junction potential corrections were not used. X-ray diffraction data were collected using a Rigaku AFC6S diffractometer. Analyses were performed by Canadian Microanalytical Services, Ltd. Melting points were determined on a Fisher-John's melting point apparatus and are uncorrected.

Preparative Details. $\text{CuCl}_2 \cdot (\text{L}1)_2$. A solution of $\text{CuCl}_2 \cdot 2\text{H}_2\text{O}$ (85 mg, 0.50 mmol) in methanol (12 mL) was heated nearly to boiling and a solution of **L2** (286 mg, 1.00 mmol) in dichloromethane (2 mL) was added. Brown crystals formed in-

stantly and after 10 minutes were separated by filtration and washed with methanol and dichloromethane. The yield is 334 mg (90%). Crystals suitable for X-ray crystallography were grown by diffusion of diethylether into dichloromethane solutions of the complex.

(CuCl₂·L2)₂. Solutions of CuCl₂·2H₂O (85 mg, 0.50 mmol) in acetonitrile (30 mL) and of L1 (173 mg, 0.50 mmol) in dichloromethane (3 mL) were mixed and the resulting deep green solution filtered. The filtrate was allowed to evaporate at room temperature. Products that formed were collected by filtration, washed with acetonitrile and dichloromethane and recrystallized from mixed dichloromethane/diethylether to give brown crystals in 75 % yield (194 mg). Diffusion of ether into dichloromethane solutions gives twinned crystals which are not suitable for X-ray studies.

CuCl₂·L3 A solution of CuCl₂·2H₂O (85 mg, 0.50 mmol) in methanol (60 mL) was added to a solution of L3 (165 mg, 0.5 mmol) in dichloromethane (3 mL). Slow evaporation of the solution gives reddish needle-like crystals which are suitable for X-ray crystallography. The yield is 188 mg (75%).

CuCl(L1)₂. A solution of CuCl₂·2H₂O (85 mg, 0.50 mmol) in methanol (60 mL) was added to a solution of L1 (286 mg, 1.0 mmol) in dichloromethane (3 mL). Slow evaporation of the solution at room temperature gave a white solid product in 75% yield (252 mg). Diffusion of ether into dichloromethane solutions of the complex gives twinned crystals which are not suitable for X-ray studies.

CuCl·L2. Method A: Solutions of CuCl₂·2H₂O (85 mg, 0.50 mmol) in ethanol (30 mL) and of L2 (173 mg, 0.50 mmol) in dichloromethane (3 mL) were mixed. After filtration, the solution was allowed to stand at room temperature and to evaporate slowly to give white solid product in 50 % yield (111 mg). **Method B:**

A solution of $(\text{CuCl}_2 \cdot \text{L2})_2$ (120 mg, 0.25 mmol) in ethanol (100 mL) was allowed to evaporate slowly at room temperature which gave white crystals with the same properties as the compound prepared by Method A.

CuSCN·L2. A solution of $\text{Cu}(\text{NO}_3)_2 \cdot 2\text{H}_2\text{O}$ (115 mg, 0.50 mmol) in ethanol (100 mL) was added to a solution of L2 (170 mg, 0.50 mmol) in dichloromethane (3 mL). A solution of NH_4SCN (152 mg, 2.0 mmol) in ethanol (10 mL) was then added and the resulting solution filtered. Slow evaporation of the filtrate gave white needle-like polycrystals in 90% yield (208 mg).

(CuBr·L3)₂. A solution of CuBr_2 (110 mg, 0.50 mmol) in ethanol (150 mL) was added to a solution of L3 (165 mg, 0.50 mmol) in dichloromethane (3 mL). Slow evaporation of the solution at room temperature gave beautiful colourless crystals suitable for X-ray studies. The yield is 137 mg (70%). Recrystallization of the compound in acetone gave $\text{CuBr} \cdot \text{L3} \cdot \text{CH}_3\text{COCH}_3$.

CuCl·L4 A solution of $\text{CuCl}_2 \cdot \text{H}_2\text{O}$ (85 mg, 0.50 mmol) in methanol (60 ml) was added to a solution of L4 (157 mg, 0.05 mmol) in dichloromethane (3 ml). Slow evaporation of the solution at room temperature gave a white solid product in 85% yield (218 mg).

Chapter 3

Molybdenum and Tungsten Carbonyl Thioether Compounds

Catalytic hydrodesulfurization is an important process both for industry and for the environment, and molybdenum and tungsten compounds have long been recognized to be good catalysts for the hydrodesulfurization processes. Thiophenes are considered to be the most difficult compounds to desulfurize for both kinetic and thermodynamic reasons [95]. Details of the mechanism of desulfurization of thiophene are unknown at present even though the technology is well established. It is however, likely that interaction between the metal and the thiophene ring is a key part of the catalytic cycle and with this in mind the thiophene-containing ligands, L1, L2, and L5 (2,5,7,10-tetrathia[12](2,5) thiophenophane [85]) have been reacted with $\text{Mo}(\text{CO})_6$ and $\text{W}(\text{CO})_6$.

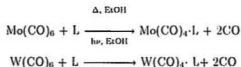
3.1 Preparation

Molybdenum or tungsten carbonyl thioether compounds were synthesized in ethanol either by thermochemical or photochemical reactions as shown below:

Table 3.1: Physical Properties and Analytical Data for Molybdenum and Tungsten Thioether Complexes

Compound	M.P. ^a (°C)	C(% (Calc)	H(% (Calc)	S(% (Calc)
Mo(CO) ₄ ·L1	125(d)	38.75 (38.86)	3.13 (2.86)	
Mo(CO) ₄ ·L2	72-73	39.08 (38.99)	2.96 (3.28)	
W(CO) ₄ ·L1	148(d)	33.10 (33.00)	2.70 (2.43)	
W(CO) ₄ ·L5	155(d)	32.22 (31.07)	3.11 (2.94)	27.03 (25.90)

^ad: Decomposition



The elemental analyses are listed in Table 3.1. and the nmr results are in Table 3.2.

While the reaction mixture is very sensitive to air, the products, once isolated, are air-stable. For molybdenum compounds, the synthesis was carried out at reflux temperatures. For the tungsten compounds, however, in addition to refluxing, uv irradiation is also needed for success in these preparations.

In spite of using vigorous conditions and excess amounts of ligand for preparation of W(CO)₄·L5, only the 1:1 complex was isolated. This is in contrast to the behaviour of macrocyclic thioethers such as 1,4,8,11-tetrathiacyclotetradecane and 1,4,7,10,13,16-hexathiacyclooctadecane which give dinuclear complexes with a bridg-

Table 3.2: Nmr Data for Molybdenum and Tungsten Thioether Carbonyl Compounds and Assignments

Compound	$\delta^1\text{H}^a$	$\delta^{13}\text{C}^a$	Assignment ^b
$\text{Mo}(\text{CO})_4\cdot\text{L}1$	7.35(2H)	126.9	1
	7.02(4H)	128.6,127.5	2,3
		137.8	4
	4.10(4H)	40.6	5
	2.70(4H)	32.2	6
$\text{Mo}(\text{CO})_4\cdot\text{L}2$	7.30(2H)	125.7,126.9	1,14
	6.98(4H)	127.2,127.5	2,3,12,13
		128.5,137.7	2,3,12,13
		141.8	4,11
	4.06(2H)	41.4	5
	4.01(2H)	40.5	10
	2.81(4H)	33.3,32.8	6,7
	2.70(2H)	31.4	8
	2.63(2H)	30.7	9
$\text{W}(\text{CO})_4\cdot\text{L}1$	7.22(2H)	126.3	1
	6.90(4H)	127.1,128.0	2,3
		137.2	4
	4.09(2H)	41.2	5
	2.70(4H)	33.5	6
$\text{W}(\text{CO})_4\cdot\text{L}5$	6.93(2H)	142,141,126,127	1,1',2,2'
	3.96(4H)	43	3,3'
	2.85(4H)	33	6,6'
	2.67(4H)	32	55'
	2.50(4H)	31	4,4'

^ain ppm from TMS.

^bPosition identification from Fig. 3.5, 3.8, 3.10.

Table 3.3: Infrared Data for Carbonyl Region of Molybdenum and Tungsten Compounds in Dichloromethane

$\nu_{CO}(\text{cm}^{-1})^a$				Assignment
$\text{Mo}(\text{CO})_4 \cdot \text{L}1$	$\text{Mo}(\text{CO})_4 \cdot \text{L}2$	$\text{W}(\text{CO})_4 \cdot \text{L}1$	$\text{W}(\text{CO})_4 \cdot \text{L}5$	
2025(m)	2025(m)	2020(m)	2019(m)	A_1
1912(b,s)	1906(b,s)	1893(b,s)	1896(b,s)	$A_1 + B_1$
1869(s)	1868(s)	1865(s)	1860(s)	B_1

^am, Medium; b, Broad; s: Strong.

ing ligand [96, 97] but coincides with that of 3,6,10,13-tetrathiabicyclo[13.4.0]nona-1,16,18-triene which forms 1:1 complex. [97, 98].

3.2 Infrared Spectroscopy

The infrared spectra of all four compounds (see Table 3.1.) were recorded in

dichloromethane. The carbonyl regions have similar peak patterns and a representative example is shown in Fig. 3.1. All data are collected in Table 3.3. The pattern of peaks is consistent with a *cis*-disubstituted $\text{L}_2\text{M}(\text{CO})_4$ species such as $\text{Mo}(\text{CO})_4 \cdot (\text{DTH})$ [99] which shows a similar pattern except that two of the bands are very close in frequency when the spectrum is observed in chloroform. Poor resolution of these bands has been reported for $\text{Mo}(\text{CO})_4 \cdot \text{en}$ in nitromethane[100]. and it seems likely therefore that the single strong broad band near 1900 cm^{-1} in the spectra of the complexes described herein is really two unresolved bands.

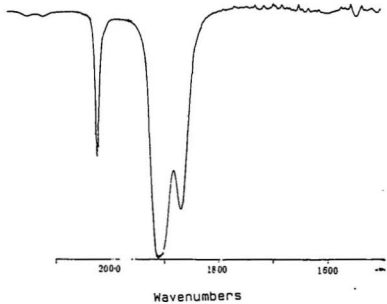


Figure 3.1: Infrared Spectra for $\text{Mo(CO)}_4 \cdot \text{L1}$ in Dichloromethane

Table 3.4: Selected Bond Lengths(Å) and Angles for W(CO)₄·L5

Distances (Å)			
W-C1	1.96(3)	W-C4	1.97(2)
W-C2	2.11(3)	W-S1	2.586(5)
W-C3	1.93(2)	W-S2	2.540(5)
Angles (deg)			
S(1)-W-S(2)	80.5(2)	S(1)-W-C(1)	86.4(9)
S(1)-W-C(2)	95.5(9)	S(1)-W-C(3)	171.5(5)
S(1)-W-C(4)	95.5(6)	S(2)-W-C(1)	91.7(7)
S(2)-W-C(2)	95.6(8)	S(2)-W-C(3)	94.4(5)
S(2)-W-C(4)	175.9(7)	C(1)-W-C(2)	172.7
C(1)-W-C(3)	87(1)	C(1)-W-C(4)	89(1)
C(2)-W-C(3)	92(1)	C(2)-W-C(4)	84(1)
C(3)-W-C(4)	89.6(8)		

3.3 X-ray Structure of W(CO)₄·L5

The PLUTO plot for W(CO)₄·L5 is shown in Fig. 3.2. The X-ray results confirm the cis-disubstituted structure proposed on the basis of infrared spectroscopy. Selected bond lengths and angles are in Table 3.4. Crystallographic data is in the Appendix.

The ligand uses only the two thioether sulfurs that are remote from the thiophene ring to coordinate to tungsten and there is no interaction between thiophene sulfur and tungsten.

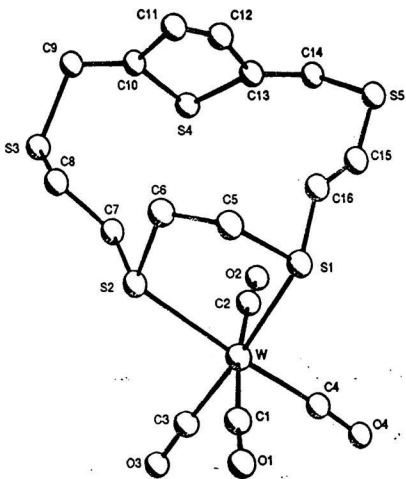


Figure 3.2: PLUTO Plot for $W(CO)_4 \cdot L5$

3.4 Dynamic Structures of Molybdenum and Tungsten Carbonyl Thioether Compounds

3.4.1 Inversion of Coordinated Sulfur

As shown by infrared spectroscopy, all these thioether complexes of molybdenum and tungsten carbonyl have a *cis*-disubstituted structure. For disubstituted complexes of this type, *meso* and *d,l* forms (Fig. 3.3) may exist in solution and are interchangeable by inversion of the coordinated sulfurs. Nmr methods are suitable for study of the inversion processes and have been applied to the thioether complexes described above.

$\text{Mo}(\text{CO})_4\cdot\text{L1}$

The nmr for $\text{Mo}(\text{CO})_4\cdot\text{L1}$ in dichloromethane (Fig. 3.4) was recorded at room temperature. The numbered structure for this compound is in Fig. 3.5. The coordinated sulfurs are asymmetric centres and so the members of each pair of hydrogens on positions 5, and 6 are nonequivalent. At room temperature in dichloromethane ^1H spectrum consists of two singlets at 4.09 and 2.67 ppm from TMS assigned to hydrogens on positions 5 and 6, respectively. This suggests fast inversion is occurring at coordinated sulphur.

To see more clearly the inversion process, nmr spectra were recorded from -80°C to $+20^\circ\text{C}$ as shown in Fig. 3.6. The nmr of this compound recorded in *d*⁸-tetrahydrofuran at room temperature shows some difference from that in dichloromethane. The methylene peak at 4.17 is broader than in dichloromethane, suggesting this is not the high temperature limiting spectrum. This means that the

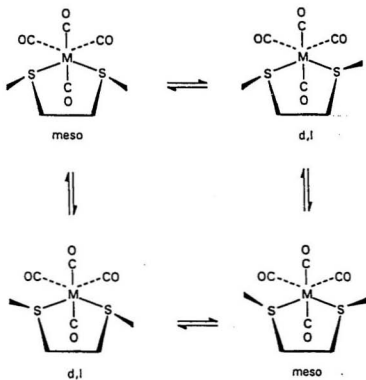


Figure 3.3: Conversion of Configuration of $M(CO)_4L$

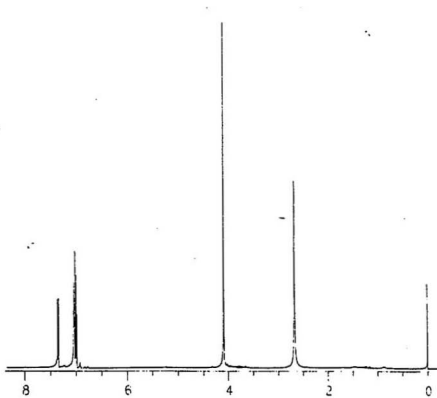


Figure 3.4: Nmr Spectra for $\text{Mo}(\text{CO})_4 \cdot \text{Li}$ in Dichloromethane at Room Temperature

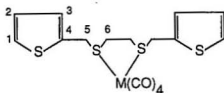


Figure 3.5: Numbered structure for $M(CO)_4L1$

inversion rate of the coordinated sulfurs in this compound is lower in THF than that in dichloromethane. The peaks of the chelate methylenes are more obviously changed. For example, the peak at 2.67 in dichloromethane becomes a major peak centered at 2.78 and a small peak at 2.68 in THF. This means that in addition to the main d,l species, the meso isomer also exists in detectable amounts in THF.

Reducing the temperature will slow the rate of inversion until at the low temperature limit, two pair of hydrogens in position 6 should become an AA'BB' system while hydrogens at position 5 become an AB system. The experimental results coincide with this expectation. As the temperature decreases, the singlet at ~ 4.0 ppm first collapses and then grows to an AB quartet at $T < -60^\circ\text{C}$. The low temperature limiting spectrum shows the presence of two isomers, d,l and meso in $\sim 4:1$ ratio, producing overlapping AB quartets centered at 4.25 and 4.28 ppm from TMS. The singlet for hydrogens in position 6 at ~ 2.8 ppm at room temperature first collapses (-20°C), then reappears as an AA'BB' pair of broad doublets centered at ~ 3.0 and 2.6 ppm ($T > 40^\circ\text{C}$). At low temperature, the chelate ring methylene hydrogens give an AA'BB' pattern consisting of two pairs of apparent doublets at 2.61 and 2.96 ppm from TMS.

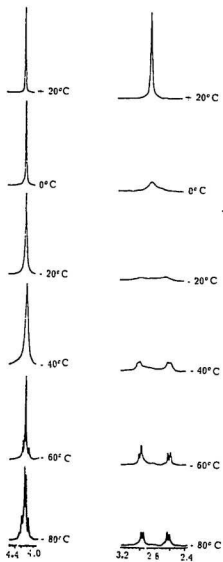


Figure 3.6: Variable Temperature ^1H nmr for $\text{Mo}(\text{CO})_4\cdot\text{L1}$ in THF

Introduction of small amounts of free ligand to the sample produces recognizable signals due to free ligand which do not change as the temperature is lowered. It is unlikely therefore that dissociation is part of the inversion process. This is in contrast to $[\text{Pd}(\text{allyl})\text{L}_5]^+$ [101] where the inversion is thought to proceed via dissociation of sulfur and to have a somewhat higher activation energy [74, 101].

It should also be noted that the chelate ring methylene hydrogens have not yet reached their limiting spectrum even at -80°C .

In conclusion, this compound undergoes rapid inversion of its metal-bound sulfurs at room temperature. The meso/d,l equilibrium is shifted towards d,l as the temperature is raised. This behavior is very similar to that of $\text{Mo}(\text{CO})_4\cdot\text{L}$ ($\text{L} = \text{bbte}$) [69, 102] and suggests that replacement of the phenyl group by thiophene does not change the inversion properties of the two chelated sulphurs significantly or in other words, interaction of thiophene with molybdenum is unlikely in this compound.

$\text{W}(\text{CO})_4\cdot\text{L1}$

The spectrum of this compound is very similar to that of the molybdenum complex except that the values of δ for the tungsten compound are slightly lower than those for molybdenum as can be seen from the data in Table 3.2. Detailed discussion will therefore be omitted.

$\text{Mo}(\text{CO})_4\cdot\text{L2}$

In this complex, there is an additional $\text{S-CH}_2\text{CH}_2$ unit compared to the L1 complex. This provides further opportunities for thiophene interaction with molybdenum as well as for 1, 4-binding site fluxionality.

The nmr spectrum for this compound in d^8 -THF is in Fig. 3.7 and the numbered structure for $\text{Mo}(\text{CO})_4\text{-L2}$ is in Fig. 3.8. Hydrogens at positions 5, 6, 7, 8, 9, and 10 all show different chemical shifts. In the free ligand, hydrogens at positions 6, 7, 8, and 9 give a singlet at ~ 2.6 ppm. Complexing usually shifts hydrogen resonances to lower field, and therefore position 9's signal should be least shifted from that of free ligand. Differentiation between 8 and 7, 6 is based on subsequent variable temperature behaviour, i.e., splitting should be similar for 6 and 7 to that found in $\text{Mo}(\text{CO})_4\text{-L1}$.

The signal due to the hydrogens at position 8 collapses at same temperature as those for the hydrogens at positions 6, and 7 and new signals grow at the same rate. Hydrogens at position 8 and 9 are an ABC_2 system. The difference in τ for the AB portion is the same as that between the A and B part of the ABCD spectrum due to 6 and 7.

The signal due to the hydrogens at position 9 collapse from the room temperature spectrum to the C_2 part of the ABC_2 system of hydrogens 8 and 9. It appears as a multiplet near 2.75 shifting with temperature to about 2.69 which partially overlaps the high field components of the signal due to positions 6, 7 and 8. Integration shows two envelopes of intensity 3 and 5 at -80°C . The meso/d,l isomer ratio seems heavily shifted in favour of one isomer as was also observed for $\text{Mo}(\text{CO})_4\text{-L1}$.

The signals due to hydrogens at positions 5 and 10 are well resolved at all temperatures studied. Hydrogens at position 5 are lower in shift than those of position 10 due to greater proximity to the metal. The meso and d,l isomers are present in almost equal amounts at room temperature as seen from the broad signal at 4.15 and a just-resolved peak at 4.04. Even at -80°C , the low temperature limiting spec-

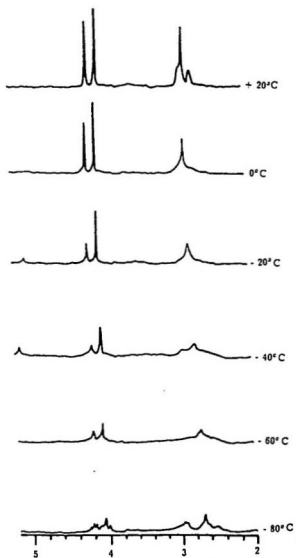


Figure 3.7: Variable Temperature ^1H nmr Spectra for $\text{Mo}(\text{CO})_4 \cdot \text{L}_2$ in $d_8\text{-THF}$

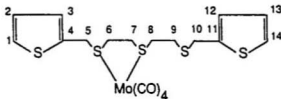


Figure 3.8: Numbered Structure for $\text{Mo}(\text{CO})_4 \cdot \text{L}2$

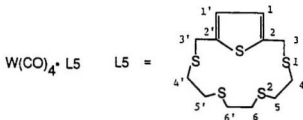


Figure 3.9: Numbered Structure for $\text{W}(\text{CO})_4 \cdot \text{L}5$

trum has not been obtained but the spectrum at -80°C shows clearly the overlap of two quartets due to non-equivalent hydrogens at positions 5 and 10. The broadness of the signal centered at 4.05 means that the *meso/d,l* equilibrium is still going on although it is very slow. This is in contrast to what is observed for $\text{Mo}(\text{CO})_4 \cdot \text{L}1$ and suggests that a larger R group is more difficult to lock in a fixed position.

$\text{W}(\text{CO})_4 \cdot \text{L}5$

The variable temperature nmr for this compound in d^8 -THF is in Fig. 3.10. and the numbered structure for this complex is in Fig. 3.9. Assignment is by comparison to the free ligand bearing in mind that coordination shifts hydrogen resonances to lower field, and by evaluation of the spectral changes with temperature. At room

temperature, the signal at ~ 7 ppm is a singlet therefore H_1 and $H_{1'}$ are equivalent. Therefore, the metal is either moving from S1, S2 coordination to S3, S4 or it is fixed on S2 and S3 and inverting. The signal at ~ 4 ppm is a singlet, therefore H_{2a} and H_{2b} and $H_{2'a}$ and $H_{2'b}$ are equivalent. This only can happen due to the movement of the metal from the top of the ring to the bottom of the ring. There is no sign of signals due to free ligand anywhere in the spectrum. Therefore the process is not a dissociative equilibrium involving full dissociation, although dissociation and inversion of one sulfur and reattachment to the metal followed by a similar sequence at the other sulfur cannot be ruled out even though it seems most unlikely. The variable temperature nmr in tetrahydrofuran shows that rapid inversion of coordinated sulfurs is the only process occurring that has a significant effect on the spectrum. It causes the signal due to hydrogens in position 3 and 3' to be a singlet at room temperature as well as exchanging the two on the two on 4, the two on 4', the two on 5, the two on 5', the two on 6 and the two on 6'. There is no 1,4-fluxional behaviour. If there were, the spectrum should show an influence of metal coordination on the shift of hydrogens in position 3(3') but it does not. Furthermore, the order of chemical shifts of hydrogens in position 4(4'), 5(5') and 6(6') should be the same as in free ligand but it is the reverse. Lowering the temperature causes the signal due to hydrogens in position 3(3') to collapse to a quartet as the inversion slows. Signals of hydrogens in position 6(6') and 5(5') collapse and then reappear as superimposed multiplets partly at ~ 3.0 and partly at ~ 2.6 ppm. The signal of hydrogens in position 4(4') collapses and grows again as a multiplet at ~ 2.75 ppm. The low temperature spectrum is a multiplet at ~ 2.5 integrating for 4H due to 2H at position 6(6') and 2H at position 6(6'), and a multiplet at $\sim 2.7(4H)$ due to

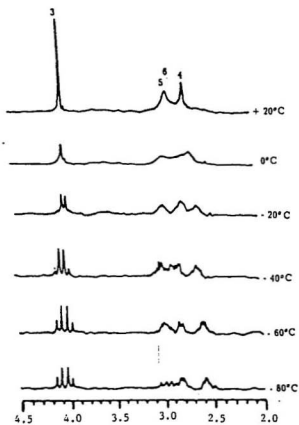


Figure 3.10: Variable Temperature ^1H nmr for $\text{W(CO)}_4 \cdot \text{L5}$ in $d^8\text{-THF}$

hydrogens at position 4(4'). Four narrowly spaced multiplets centred at ~ 3.0 ppm from TMS are due to the other 2H of position 6(6') and the other 2H of position 5(5').

In contrast to the inversion processes discussed in earlier sections, this complex has its inversion stopped at a relatively higher temperature (-20°C) compared to that (-60°C) observed for the molybdenum compounds. This might reflect the effect of the metal on the activation energy of inversion. Throughout the temperature range studied only singlets at ~ 7.0 and ~ 4.0 ppm are observed. This clearly indicates that one isomer is preferred. By comparing with the X-ray structure studies, which showed that only the meso isomer is present in the solid state, it seems likely that in tetrahydrofuran, at least up to 20°C , the compound is dominated by one isomer and that is the meso form.

Comparing $\text{Mo}(\text{CO})_4\cdot\text{L1}$, $\text{Mo}(\text{CO})_4\cdot\text{L2}$, $\text{W}(\text{CO})_4\cdot\text{L1}$ and $\text{W}(\text{CO})_4\cdot\text{L5}$, it seems that these compounds would all show a preference for the meso isomer. As for $\text{W}(\text{CO})_4\cdot\text{L5}$, due to rigidity of the compound, it can be detected by nmr in only one isomeric form (meso). In $\text{Mo}(\text{CO})_4\cdot\text{L1}$ and $\text{W}(\text{CO})_4\cdot\text{L1}$, the meso isomer is still stable enough to play a major part in solution. For $\text{Mo}(\text{CO})_4\cdot\text{L2}$, due to steric effects, the meso isomer is destabilized compared to the d,l isomer and significant amounts of both isomers may be detected. The d,l \rightleftharpoons meso equilibrium is still going on, even at -80°C .

Solvent effects on the inversion processes were also examined but no significant difference in spectral characteristics was observed. This suggests that dissociation of coordinated sulfur is unlikely to be part of the inversion process.

3.4.2 Fluxionality

The ^1H nmr spectrum of $\text{Mo}(\text{CO})_4\text{-L2}$ was examined in d^8 -toluene. This allowed higher temperatures to be achieved than was possible in either THF or dichloromethane which were used as solvents in the inversion studies. In those solvents, no evidence for a 1,4-binding site fluxionality could be seen. The results in toluene, however, reveal such a process and are displayed in Fig. 3.11. At low temperature, the behaviour of the compound is similar to that when it is dissolved in tetrahydrofuran. At -90°C , the spectrum is that expected from overlap of spectra from the meso and d,l isomers. Signals due to the thiophene remote from the metal are still well resolved. At -90°C , hydrogens in position 5 (see Fig. 3.8) show clearly as an AB quartet. Hydrogens in position 10 still give a singlet, although the signal is broad. As the temperature rises to 10°C , signals of hydrogens in position 5 and 10 are both sharp singlets, and the six thiophene hydrogens are also well resolved. As the temperature rises to 80°C , significant changes occur. Two well separated signals belonging to hydrogens on positions 5 and 10 collapse to one singlet which indicates that the metal moves between all three sulphurs. This is the first example of a 1,4-binding site fluxionality for acyclic ligands containing nitrogen, phosphorus, oxygen or sulfur heteroatoms as donors. Separate signals for hydrogens in positions 6, 7, 8, and 9 cannot be distinguished throughout the temperature range. The only change that occurs as the temperature increases is that the signal grows and at very high temperature, the signal becomes more sharp than at low temperature.

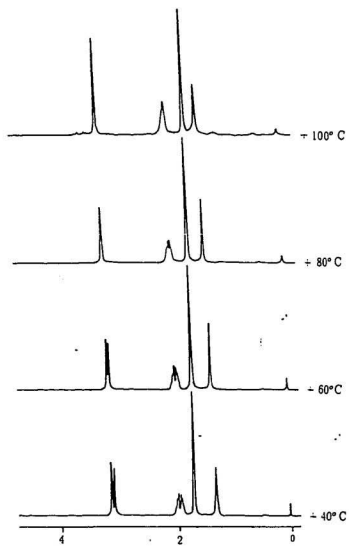


Figure 3.11: Variable Temperature ^1H nmr for $\text{Mo(CO)}_4\cdot\text{L2}$ in d^8 -Toluene Solution

3.5 Conclusion

All these compounds show rapid inversions of coordinated sulfur atoms at room temperature. The replacement of a phenyl group by a thiophene, addition of one more thioether sulphur in the ligand and building the thioether sulphur into a macrocyclic ring do not effect the inversion process significantly as all the inversions are rapid at room temperature. The inversion is, however, stopped at a higher temperature for $W(CO)_4 \cdot L5$ than for others. There is also a difference in d,l/meso isomer equilibrium. The macrocyclic thioether complexes exist only in the meso form. The open chain thioether compounds exist in two forms throughout the temperature range studied although presumably d,l isomers will dominate at low temperature. The steric bulk of the ligands also affects the d,l/meso equilibrium. Steric effects on the 1,4-fluxional process cannot be observed due to decomposition of $W(CO)_4 \cdot L5$ at higher temperature. This observation of fluxionality in $Mo(CO)_4 \cdot L2$ represents the first report of the 1,4 fluxional process on an open chain ligand containing nitrogen, phosphorus, oxygen or sulfur as donor atoms.

3.6 Experimental

Materials All commercially available starting materials were obtained from the Aldrich Chemical Co. Inc. and were used without further purification. Preparation of L5 was carried out by the reported method [85].

Spectroscopic data were obtained by using the same instruments as described in previous experimental section of this thesis.

$Mo(CO)_4 \cdot L1$. Molybdenum hexacarbonyl (130 mg, 0.492 mmol) and L1 (140

mg, 0.489 mmol) were added to commercial absolute ethanol (15 mL) and the mixture was refluxed under nitrogen for 4 hours. The yellow precipitate that formed was separated, washed with ethanol and then diethylether and dried in air: yield 205 mg (85 %).

Mo(CO)₄-L2. This preparation was similar to that for its L1 analog except that the product did not precipitate from the reaction mixture. Instead, the mixture was filtered and the filtrate was added to an equal volume of hexane. This solution was allowed to evaporate slowly giving yellow crystals: yield 177 mg (65 %).

W(CO)₄-L1. Tungsten hexacarbonyl (350 mg, 1.00 mmol) and L1 (140 mg, 0.489 mmol) were dissolved in commercial absolute ethanol (150 mL). The solution was irradiated with a 100 W Hanovia uv lamp and refluxed for 8 hours under nitrogen. A yellow precipitate was separated from the cooled solution and washed with ethanol and then diethylether. The solid was placed in a sublimator and unreacted W(CO)₆ removed *in vacuo*. The remaining solid was chromatographed on SiO₂ using dichloromethane as eluant: yield 146 mg (50 %).

W(CO)₄-L5. This preparation was similar to that of the L1 analog except that irradiation and refluxing were continued for 36 hours: yield 247 mg (80 %).

Bibliography

- [1] Colman, P.M.; Freeman, H.C.; Guss, J.M.; Mutara, M.; Norris, V.A.; Ranshaw, J.A.M.; Venkatappa, M.P. *Nature* **1978**, *272*, 319.
- [2] Freeman, H.C. *Proc. Int. Conf. Coord. Chem.*, *21st* **1980**, p 8.
- [3] Setzer, W.N.; Ogle, C.A.; Wilson, G.S.; Glass, R.S. *Inorg. Chem.* **1983**, *22*, 266.
- [4] Clarkson, J.A.; Yagbasan, R.; Blower, P.J.; Cooper, S.R. *J. Chem. Soc., Chem. Commun.* **1989**, 1244.
- [5] Pett, V.B.; Diaddario, L.L.; Dockal, E.R.; Corfield, P.W.; Ceccarelli, C.; Glick, M.D.; Ochrymowycz, L.A.; Rorabacher, D.B. *Inorg. Chem.* **1983**, *22*, 3661.
- [6] Diaddario, L.L.; Dockal, E.R.; Glick, M.D.; Ochrymowycz, L.A.; Rorabacher, D.B. *Inorg. Chem.* **1985**, *24*, 356.
- [7] Glick, M.D.; Gavel, D.P.; Diaddario, L.L.; Rorabacher, D.B. *Inorg. Chem.* **1976**, *15*, 1190.
- [8] Dockal, E.R.; Diaddario, L.L.; Glick, M.D.; Rorabacher, D.B. *J. Am. Chem. Soc.* **1977**, *99*, 4530.

- [9] Corfield, P.W.R.; Ceccarelli, C.; Glick, M.D.; Moy, I.W.Y.; Ochrymowycz, L.A.; Korabacher, D.B. *J. Am. Chem. Soc.* **1985**, *107*, 2399.
- [10] Hartman, J.R.; Cooper, S.R. *J. Am. Chem. Soc.* **1986**, *108*, 1202.
- [11] Cooper, S.R.; Rawle, S.C. *Struct. Bonding* **1990**, *72*, 1.
- [12] DeSimone, R.E.; Glick, M.D. *J. Am. Chem. Soc.* **1976**, *98*, 762.
- [13] Grant, G.J.; Grant, C.D.; Setzer, W.N. *Inorg. Chem.* **1991**, *30*, 353.
- [14] Glass, R.S.; Wilson, G.S.; Setzer, W.N. *J. Am. Chem. Soc.* **1980**, *102*, 5068.
- [15] Dale, J. *Acta Chem. Scand.* **1973**, *27*, 1115.
- [16] Setzer, W.N.; Cacioppo, E.L.; Guo, Q.; Grant, G.J.; Kim, D.D.; Hubbard, J.L.; VanDerveer, D.V. *Inorg. Chem.* **1990**, *29*, 2672.
- [17] Setzer, W.N.; Afshar, S.; Burns, N.L.; Ferrante, L.A.; Hester, A.M.; Meehan, E.J. Jr.; Grant, G.J.; Isaac, S.M.; Laudeman, C.P.; Lewis, C.M. *Heteroat. Chem.* **1990**, *1*, 375.
- [18] Wolf, R.E., Jr.; Hartman, J.R.; Storey, J.M.E.; Foxman, B.M.; Cooper, S.R. *J. Am. Chem. Soc.* **1987**, *109*, 4328.
- [19] Rawle, S.C.; Admans, G.A.; Cooper, S.R. *J. Chem. Soc., Dalton Trans.* **1988**, 93.
- [20] Rawle, S.C.; Yagbasan, R.; Prout, K.; Cooper, S.R. *J. Am. Chem. Soc.* **1987**, *109*, 6181.

- [21] Blake, A.J.; Gould, R.O.; Holder, A.J.; Hyde, T.I.; Schroder, M. *J. Chem. Soc., Dalton Trans.* **1988**, 1861.
- [22] Kuppers, H.; Wieghardt, K. *Polyhedron* **1989**, *8*, 1770.
- [23] Wieghardt, K.; Kuppers, H.; Weiss, J. *Inorg. Chem.* **1985**, *24*, 3067.
- [24] Kuppers, H.; Neves, A.; Pomp, C.; Ventur, D.; Wieghardt, K.; Nuber, B.; Weiss, J. *Inorg. Chem.* **1986**, *25*, 2400.
- [25] Bell, M.N.; Blake, A.J.; Kuppers, H.; Schroder, M.; Wieghardt, K. *Angew. Chem. Int. Ed. Engl.* **1987**, *26*, 250.
- [26] Cooper, S.R. *Acc. Chem. Res.* **1988**, *21*, 141.
- [27] Blake, A.J.; Holder, A.J.; Hyde, T.I.; Schroder, M. *J. Chem. Soc., Chem. Commun.* **1987**, 987.
- [28] Ashby, M.T.; Lichtenberger, D.L. *Inorg. Chem.* **1984**, *24*, 636.
- [29] Blake, A.J.; Holder, A.J.; Hyde, T.I.; Kuppers, H.; Schroder, M.; Stotzel, S.; Wieghardt, K. *J. Chem. Soc., Chem. Commun.* **1989**, 1600.
- [30] Blake, A.J.; Holder, A.J.; Hyde, T.I.; Schroder, M. *J. Chem. Soc., Chem. Commun.*, **1989**, 1433.
- [31] Addison, A.W. in Karlin K.D.; Zubieta, J., Eds. "Copper Coordination Chemistry: Biochemical and Inorganic Perspectives", Adenine Press, Guilderland, N.Y. **1983**.

- [32] Dockal, E.R.; Jones, T.E.; Sokol, W.F.; Engerer, R.J.; Rorabacher, D.B.; Ochrymowycz, L.A. *J. Am. Chem. Soc.* **1976**, *98*, 4322.
- [33] Jones, T.E.; Rorabacher, D.B.; Ochrymowycz, L.A. *J. Am. Chem. Soc.* **1975**, *97*, 7485.
- [34] Cabral, M.F.; Cabral, J.O.; Bouwman, E.; Driessen, W.L.; Reedijk, J. *Inorg. Chim. Acta* **1990**, *167*, 205.
- [35] Pavlishchuk, V.V.; Yatsimirskii, K.B.; Strizhak, P.E.; Labuda, J. *Inorg. Chim. Acta* **1989**, *164*, 65.
- [36] Rorabacher, D.B.; Bernardo, M.M.; Vande Linde, A.M.Q.; Leggett, G.H.; Westerber, B.C.; Martin, M.J.; Ochrymowycz, L.A. *Pure and Appl. Chem.* **1988**, *60*, 501.
- [37] Siegfried, E.; Kaden, T.A. *Helv. Chim. Acta* **1984**, *67*, 29.
- [38] Gisselbrecht, J.P.; Gross, M., *Electrochemical and Spectrochemical Studies of Biological Redox Compounds*, Adv. Chem. Ser., 201, Am. Chem. Soc., New York, **1982**, p.109.
- [39] Endicot, J.F.; Durham, B. in Melson, G.A.(ed.), *Coordination Chemistry of Macrocyclic Compounds*, Plenum, New York, **1979**, p. 413.
- [40] Sakaguchi, U; Addison, A.W. *J. Chem. Soc., Dalton Trans* **1979**, 600.
- [41] James, B.R.; Williams, R.J.P., *J. Chem. Soc.* **1961**, 2007.
- [42] Hawkins, C.J.; Perrin, D.D. *J. Chem. Soc* **1962**, 1351.

- [43] Wathrich, K. *Helv. Chim. Acta* **1966**, *49*, 1400.
- [44] Martin, J.M.; Endicott, J.F.; Ochrymowycz, L.A.; Rorabacher, D.B. *Inorg. Chem.* **1987**, *26*, 3012.
- [45] Fee, J.A. *Struct. Bonding* **1975**, *23*, 1.
- [46] Osterberg, R. *Coord. Chem. Rev.* **1974**, *12*, 309.
- [47] Beinert, H.; *Coord. Chem. Rev.* **1977**, *23*, 119.
- [48] Hathaway, B.J.; Billing, D.E. *Coord. Chem. Rev.* **1970**, *5*, 137.
- [49] Hathaway, B.J.; Tomlinson, A.A.G. *Coord. Chem. Rev.* **1970**, *5*, 1.
- [50] Yokoi, H.; Addison, A.W. *Inorg. Chem.* **1977**, *16*, 1341 and refs. therein.
- [51] Peisach, J.; Blumberg, W.E. *Arch. Biochem. Biophys.* **1974**, *165*, 691.
- [52] Reinen, D.; Ozarowski, A.; Jakob, B.; Pebler, J.; Stratemeier, H. Wiegardt, K.; Tolksdorf, I. *Inorg. Chem.* **1987**, *26*, 4010.
- [53] Hartman, J.R.; Cooper, S.R. *J. Am. Chem. Soc.* **1986**, *108*, 1202.
- [54] Davis, P.H.; White, K.L.; Belford, R.L. *Inorg. Chem.* **1975**, *14*, 1753.
- [55] Miyamoto, R.; Ohba, Y.; Iwaizumi, M., *Inorg. Chem.*, **1990**, *29*, 3234.
- [56] Bouwman, E.; Driessen, W.L.; Reedijk, J.; Smykalla, C.; Smits, J.M.M.; Beurskens, P.T.; Laschi, F.; Zanello, P. *Inorg. Chem.* **1990**, *29*, 4881.
- [57] Abel, E.W.; Bush, R.P.; Hopton, F.J.; Jenkins, C.R. *J. Chem. Soc., Chem. Commun.* **1966**, 58.

- [58] Orrell, K.G. *Coord. Chem. Rev.* **1989**, *96*, 1.
- [59] Abel, E.w.; Bhargava, S.K.; Orrell, K.G., *Prog. Inorg. Chem.* **1984**, *32*, 1.
- [60] Barker, E.F. *Phys. Rev.* **1929**, *33*, 684.
- [61] Dennison, D.M.; Hardy, J.D. *Phys. Rev.* **1932**, *39*, 938.
- [62] Mislow, K. *Rec. Chem. Progr.* **1967**, *28*, 217.
- [63] Abel, E.W.; Khan, A.R.; Kite, K.; Orrell, K.G.; Sik, V. *J. Chem. Soc., Dalton Trans.* **1980**, 2208.
- [64] Cross, R.J.; Green, T.H.; Keat, R. *J. Chem. Soc., Chem. Commun.* **1974**, 207.
- [65] Cross, R.J.; Green, T.H.; Keat, R. *J. Chem. Soc., Dalton Trans.* **1976**, 1150.
- [66] Cross, R.J.; Dalgleish, I.G.; Smith, G.J.; Wardle, R. *J. Chem. Soc., Dalton Trans* **1972**, 992.
- [67] Cross, R.J.; Green, T.H.; Keat, R. *J. Chem. Soc., Chem. Commun.* **1974**, 207.
- [68] Donaldson, R.; Hunter, G.; Massey, R.C. *J. Chem. Soc., Dalton Trans* **1974**, 288.
- [69] Hunter, G.; Massey, R.C. *J. Chem. Soc., Dalton Trans* **1976**, 2007.
- [70] Schenk, W.A.; Schmidt, M. *Z. Anorg. Allg. Chem* **1975**, *416*, 311.
- [71] Binsch, G.; Kleier, D.A. *Program 140, Quantum Chemistry Program Exchange Indiana University, IN*, **1969**.

- [72] Sandstrom, J. *Dynamic NMR Spectroscopy* Academic Press, London, 1982.
- [73] Sundquist, W.I.; Ahmed, K.J.; Hollis, L.S.; Lippard, S.J. *Inorg. Chem.* 1987, 26, 1524.
- [74] Liu, S.; Lucas, C.R.; Newlands, M.J.; Charland, J-P. *Inorg. Chem.* 1990, 29, 4380.
- [75] Hunter, G.; McAuley, A.; Whitcombe, T.W. *Inorg. Chem.* 1988, 27, 2634.
- [76] Abel, E.W.; Booth, M.; Orrell, K.G.; Pring, G.M. *J. Chem. Soc., Dalton Trans.* 1981, 1944.
- [77] Abel, E.W.; King, G.D.; Orrell, K.G.; Pring, G.M.; Sik, V.; Cameron, T.S. *Polyhedron* 1983, 2, 1117.
- [78] Abel, E.W.; Bhargava, S.K.; MacKenzie, T.E.; Mittal, P.K.; Orrell, K.G.; Sik, V. *J. Chem. Soc., Chem. Commun.* 1982, 983.
- [79] Abel, E.W.; Bhargava, S.K.; Mittal, P.K.; Orrell, K.G.; Sik, V. *J. Chem. Soc., Chem. Commun.* 1982, 535.
- [80] Blicke, F.F.; Burckhalter, J.H. *J. Am. Chem. Soc.*, 1942, 64, 477.
- [81] Guss, J.M.; Freeman, H.C. *J. Mol. Biol.*, 1983, 169, 521.
- [82] Adman, E.T.; Jensen, L.H.; *Isr. J. Chem.*, 1981, 21, 8.
- [83] Norris, G. E.; Anderson, B.F.; Baker, E.N. *J. Am. Chem. Soc.*, 1986, 108, 2784.

- [84] Baker, E.W.; Norris, G.E. *J. Chem. Soc., Dalton Trans.* **1977**, 877.
- [85] Lucas, C.R.; Liu, S.; Thompson, L.K. *Inorg. Chem.* **1990**, *29*, 85.
- [86] Murray, S.G.; Hartley, F.R. *Chem. Rev.* **1981**, *81*, 365.
- [87] Hall, D.; Mckinnon, A.J.; Waters, T.N. *J. Chem. Soc.* **1965**, 425.
- [88] Mckinnon, A.J.; Waters, T.N.; Hall, D. *J. Chem. Soc.* **1964**, 3290.
- [89] Johnson, D.R.; Watson, W.H. *Inorg. Chem.* **1971**, *10*, 1069, 1281.
- [90] Lucas, C.R.; Liu, S.; Newlands, M.J.; Charland, J.P.; Gabe, E.J. *Can. J. Chem.* **1989**, *67*, 639.
- [91] Lever, A.B.P. *Inorganic Electronic Spectroscopy 2nd ed.* Elsevier, Amsterdam. **1984** pp. 554-569.
- [92] Lucas, C.R. unpublished results.
- [93] Feltham, R.D.; Hayter, R.G. *J. Chem. Soc.* **1964**, 4587.
- [94] Von Deuten, K; Kopf, J.; Klar, G. *Cryst. Struct. Commun.* **1979**, *8*, 721.
- [95] Belen'kii, L.I. in Belen'kii, L.I.(ed.), *Chemistry of Organosulfur Compounds*, West Sussex, England, **1990**, p 193.
- [96] Young, C.G.; Broomhead, J.A.; Boreham, C.J. *J. Organometallic Chem.* **1984**, *260*, 91.
- [97] Grant, G.J.; Carpenter, J.P.; Setzer, W.N.; VanDerveer, D.G.; *Inorg. Chem.* **1989**, *28*, 4128.

- [98] Groot, B.; Loeb, S.J. *Inorg. Chem.* **1990**, *29*, 4084.
- [99] Dobson, G.R.; Stolz, I.W.; Sheline, R.K. *Adv. Inorg. Radiochem.* **1966**, *8*, 1.
- [100] Cotton, F.A.; Kraihanzel, C.S., *Inorg. Chem.* **1963**, *2*, 536.
- [101] Lucas, C.R.; Liu, S.; Newlands, M.J.; Gabe, E.J. *Can. J. Chem.* **1990**, *68*, 1357.
- [102] Cross, R.J.; Hunter, G.; Massey, R.C. *J. Chem. Soc., Dalton Trans.* **1976**, 2015.
- [103] Abel, E.W.; Booth, M.; Orrell, K.G.; Pring, G.M.; Cameron, T.S. *J. Chem. Soc., Chem. Commun.* **1981**, 29.
- [104] Abel, E.W.; Hutson, G.V. *J. Inorg. Nucl. Chem.* **1969**, *31*, 3333.
- [105] Bouwman, E.; Driessen, W.L.; Reedijk, J. *Coord. Chem. Rev.* **1990**, *104*, 143.

Appendix A

Crystallographic Data

Table A.1: Crystallographic Data for $\text{CuCl}_2 \cdot 2\text{L1}$

Parameter	Value
Chemical Formula	$\text{C}_{12}\text{H}_{14}\text{Cl}_2\text{Cu}$
M	420.93
Crystal System	Monoclinic
Space Group n	$\text{P}2_1/\text{a}(\#14)$
a/Å	13.586(2)
b/Å	7.7881(6)
c/Å	14.899(3)
β /deg	102.29(1)
$D_c/\text{g cm}^{-3}$	1.815
Z	4
Radiation($\text{MoK}_{\alpha\text{beta}}$), $\lambda/\text{Å}$	0.71069
F(000)	852
μ/cm^{-1}	22.75
Crystal Size/mm	$0.350 \times 0.200 \times 0.100$
No. of Reflections Collected	3067
2θ Range	25
$R(F_o^2)$	0.043
$R_w(F_o^2)$	0.042
Goodness of Fit	1.87
No. of Variables	200
Temperature/deg	26
Scan Rate/ $^\circ \text{min}^{-1}$	32.0

Table A.2: Crystallographic Data for CuCl₂·L3

Parameter	Value
Chemical Formula	C ₁₄ H ₁₈ Cl ₂ OS ₄ Cu
M	464.99
Crystal System	Orthorhombic
Space Group	Pnma (#62)
a/Å	12.562
b/Å	17.435
c/Å	8.767
D _c /g cm ⁻³	1.608
Z	4
Radiation(MoK _{α1}), λ/Å	0.71069
F(000)	948
μ/cm ⁻¹	18.37
Crystal Size/mm	0.400 × 0.080 × 0.080
No. of Reflections Collected	1972
2θ Range	21
R(F _o ²)	0.050
R _w (F _o ²)	0.043
Goodness of Fit	1.60
No. of Variables	106
Temperature/deg	26
Scan Rate/° min ⁻¹	8.0

Table A.3: Crystallographic Data for CuBr-L3

Parameter	Value
Chemical Formula	C ₁₄ H ₁₈ BrOS ₄ Cu
M	473.99
Crystal System	Monoclinic
Space Group	P2 ₁ /n (#14)
a/Å	9.982(2)
b/Å	19.103(2)
c/Å	10.738(2)
β /deg	115.53 (1)
D _c /g cm ⁻³	1.704
Z	4
Radiation(MoK _{alpha}), λ /Å	0.71069
F(000)	952
μ /cm ⁻¹	37.57
Crystal Size/mm	0.350 × 0.200 × 0.150
No. of Reflections Collected	3575
2 θ Range	25
R(F _o ²)	0.052
R _w (F _o ²)	0.046
Goodness of Fit	2.30
No. of Variables	194
Temperature/deg	26
Scan Rate/° min ⁻¹	16.0

Table A.4: Crystallographic Data for $W(CO)_4 \cdot L5$

Parameter	Value
Chemical Formula	$C_{16}H_{18}O_4S_5W$
M	618.47
Crystal System	Monoclinic
Space Group n	Cc(no. 9)
a/Å	9.672(4)
b/Å	14.777(2)
c/Å	15.123(2)
β /deg	99.56(2)
D_c /g cm ⁻³	1.927
Z	4
Radiation(MoK α), λ /Å	0.71069
F(000)	1200
μ /cm ⁻¹	60.24
Crystal Size/mm	0.350 × 0.200 × 0.200
No. of Reflections Collected	2079
2θ Range	25
$R(F_o^2)$	0.036
$R_w(F_o^2)$	0.027
Goodness of Fit	2.05
No. of Variables	233
Temperature/deg	26
Scan Rate/° min ⁻¹	16.0

